Universidade de Aveiro Departamento de Química
2009

Cláudia Leonor Santos Louros

Extracção de Biomoléculas com Sistemas Aquosos Bifásicos

Extraction of Biomolecules with Aqueous Two Phases Systems

Universidade de Aveiro Departamento de Química
2009

Cláudia Leonor Santos Louros

Extracção de Biomoléculas com Sistemas Aquosos Bifásicos

Extraction of Biomolecules with Aqueous Two Phases Systems

Dissertação apresentada à Universidade de Aveiro para cumprimento dos requisitos necessários à obtenção do grau de Mestre em Materiais Derivados de Recursos Renováveis, realizada sob a orientação científica do Professor Dr. João Manuel da Costa e Araújo Pereira Coutinho, Professor Associado com Agregação do Departamento de Química da Universidade de Aveiro e co-orientação de Dra. Mara Guadalupe Freire Martins, Estagiária de Pós-Doutoramento no Instituto de Tecnologia Química e Biológica, ITQB2, Universidade Nova de Lisboa.

Dedico este trabalho a todos os que me apoiaram.

o júri

Presidente

Prof. Doutor Armando Jorge Domingues Silvestre
Professor Associado com Agregação da Universidade de Aveiro

Prof. Doutor João Manuel da Costa e Araújo Pereira Coutinho
Professor Associado com Agregação da Universidade de Aveiro

Prof. Doutor Luís Manuel das Neves Belchior Faia dos Santos
Professor associado da Faculdade de Ciências da Universidade do Porto

Doutora Mara Guadalupe Freire Martins
Estagiária de Pós-Doutoramento no Instituto de Tecnologia Química e Biológica, ITQB2, Universidade Nova de Lisboa

agradecimentos

Agradeço à minha família por entender todas a decisões que tomei. Ao Renato pela paciência, compreensão e pelo apoio incondicional. À Rosa por me ajudar, estando sempre presente a qualquer hora. Aos meus amigos que nunca se esqueceram e sempre me apoiaram.

Agradeço ao meu orientador Prof. Dr. João Coutinho pela oportunidade que me deu, à minha co-orientadora Dra. Mara Freire pelo apoio, pela ajuda incansável e por acreditar em mim. Principalmente pela ajuda a nível de percepção e interpretação de resultados e por todas as correcções que contribuíram para o meu crescimento profissional.

A todos os membros do grupo "PATh" (Pedro Carvalho, Maria Jorge, Sónia Ventura, Mariana Belo, Carla Gonçalves, Bernd, Luciana, Mayra, Ana Caço), por serem um grupo magnífico, onde podia sempre recorrer em qualquer situação, principalmente à Sónia Ventura pelo apoio, pela ajuda e aventura da noite perdida ao tentarmos recuperar os ficheiros perdidos duas vezes seguidas.

Ao grupo da salinha mini-PATh: Ritinha, Jorge, Marise, Catarina, Sofia, Ruti, Mariana, Samuel, Jeannette, podia sempre contar com eles. Agradeço à Catarina pela ajuda e explicações para o aperfeiçoamento do método, onde eu sempre podia recorrer em qualquer dúvida, e pelas discussões de resultados para o melhor entendimento.

Por todos os dias de trabalho, que eram um desafio constante. A horinha do café, pelo convívio do grupo, por todos os bolos que houve na hora do lanche...
Agradeço pelos amigos que fiz.

palavras-chave

Sistemas aquosos bifásicos, líquidos iónicos, hidratos de carbono, coeficiente de partição, extracção, biomoléculas.

resumo

Os líquidos iónicos (LIs) representam uma nova classe de solventes iónicos com pressões de vapor desprezáveis o que os torna potenciais substitutos para compostos orgânicos voláteis que são actualmente utilizados. Para além disso, a combinação selectiva do catião e do anião permite afinar as suas propriedades termofísicas e a sua capacidade de solvatação/extracção.

Os sistemas aquosos bifásicos (SAB) são considerados uma alternativa rentável e eficaz para a extracção, recuperação e purificação de diversas biomoléculas.

Neste trabalho, traçaram-se os diagramas de fases de sistemas compostos por líquido iónico + sal inorgânico + água e líquido iónico + hidratos de carbono + água, à temperatura de 298 K e pressão atmosférica.

Para além do interesse em SAB baseados em LI e sais inorgânicos, a aplicação de hidratos de carbono para substituir os sais inorgânicos em sistemas de elevada carga iónica aparenta ser uma abordagem mais benéfica.

Os dois tipos de SAB estudados foram avaliados no que respeita à sua capacidade para extracção de biomoléculas. As biomoléculas seleccionadas comportam aminoácidos, corante alimentares e alcalóides. Os SAB compostos por LIs demonstraram ser uma potencial abordagem para a extracção de biomoléculas em processos biotecnológicos.

keywords

Aqueous two phase systems, ionic liquids, carbohydrates, partition coefficient, extraction, biomolecules.

abstract

Ionic liquids (ILs) represent a new class of ionic solvents that exhibit negligible vapour pressures and that further makes them potential substitutes for the volatile organic compounds currently employed. Moreover, the selection of both the cation and anion and, therefore, the possibility of fine-tunning their thermophysical properties and solvation/extraction performance, is an extremely important feature.

Aqueous biphasic systems (ATPS) are considered attractive alternatives for the extraction, recovery and purification of several biomolecules.

In this work, phase diagrams composed by ionic liquid + inorganic salt + water, at 298 K and atmospheric pressure, were determined.

Besides the interest on IL-based ATPS with inorganic salts, the application of carbohydrates to substitute those highly charged systems seems to be a more benign approach.

Both type of ATPS were evaluated trough their extraction capability for biomolecules. The selected biomolecules include amino acids, food colourings and alkaloids. ILs-based ATPS have shown to be a prospective extraction media for biomolecules in biotechnological processes.

Contents

Notation

List of Symbols

σ	Standard deviation
R^2	Correlation coefficient
K_i	Partitioning coefficient of solute *i*
w_s	Mass fraction of salt or carbohydrate
X	Mass fraction of salt or carbohydrate
w_{IL}	Mass fraction of ionic liquid
Y	Mass fraction of ionic liquid

List of Abbreviations

ATPS	Aqueous Two Phase Systems
CH	Carbohydrate
IL	Ionic Liquid
RTIL	Room Temperature IL
TL	Tie Line
TLL	Tie Line Length
UV-Vis	Ultra-Violet Visible
NMR	Nuclear Magnetic Resonance
K_3PO_4	Potassium triphosphate
$[\beta carot]_{IL}$	Concentration of β-carotene in the IL-rich aqueous phase
$[\beta carot]_{K3PO4}$	Concentration of β-carotene in the K_3PO_4-rich aqueous phase
$[Caf]_{IL}$	Concentration of caffeine in the IL-rich aqueous phase
$[Caf]_{K3PO4}$	Concentration of caffeine in the K_3PO_4-rich aqueous phase
$[Trp]_{IL}$	Concentration of L-tryptophan in the IL-rich aqueous phase
$[Trp]_{K3PO4}$	Concentration of L-tryptophan in the K_3PO_4-rich aqueous phase
$[Rhod]_{IL}$	Concentration of rhodamine 6G in the IL-rich aqueous phase
$[Rhod]_{K3PO4}$	Concentration of rhodamine 6G in the K_3PO_4-rich aqueous phase
$[Trp]_{CH}$	Concentration of L-tryptophan in the CH-rich aqueous phase
$[C_2mim][MeSO_4]$	1-ethyl-3-methylimidazolium methylsulfate
$[C_4mim][Cl]$	1-butyl-3-methylimidazolium chloride
$[C_4mim][BF_4]$	1-butyl-3-methylimidazolium tetrafluoroborate
$[C_4mim][HSO_4]$	1-butyl-3-methylimidazolium hydrogenosulfate
$[C_4mim][CF_3SO_3]$	1-butyl-3-methylimidazolium trifluoromethanesulfonate
$[C_6mim][Cl]$	1-hexyl-3-methylimidazolium chloride
$[C_7H_7mim][Cl]$	1-benzyl-3-methylimidazolium chloride
Choline Chloride	2-hydroxyethyltrimethylammonium chloride
CYPHOS IL 106	Triisobutyl(methyl)phosphonium tosylate
CYPHOS IL 108	Tributyl(methyl)phosphonium methylsulfate
CYPHOS IL 163	Tetrabutylphosphonium bromide

List of Tables

List of Figures

1. Introduction

1.1. Ionic Liquids

Room temperature ionic liquids (RTILs) are organic salts with melting points at or below room temperature. Typically, RTILs consist of large nitrogen- or phosphorus-containing organic cations (such as quaternary ammonium, pyridinium, piperidinium, pyrrolidinium, imidazolium and phosphonium-based, among others) and an organic or inorganic anion[1]. Figure 1 presents the molecular structure of a common IL.

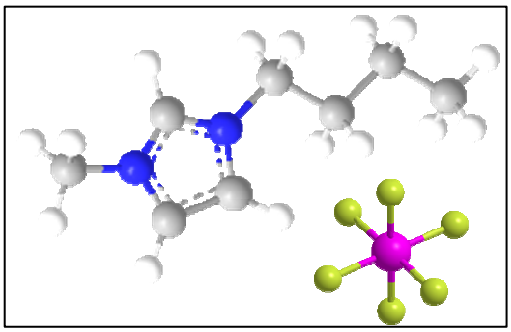

Figure 1 - Molecular structure of [C_4mim][PF_6], 1-butyl-3-methylimidazolium hexafluorophosphate.

Due to the ILs non volatility, high stability, large liquidus range and good solvation properties for both, polar and nonpolar, as well as inorganic compounds, they are attractive as solvents for chemical reactions and separations. With these unique features, ILs have gained increased attention in academia and industrial research and are nowadays suggested as interesting alternatives for volatile and non-benign organic solvents in numerous fields[2, 3]. Indeed, these particular characteristics contributed to their classification as "green" solvents. This categorization yielded a growth of their applications in organic synthesis, catalysis, and separations of polymer science, including chromatography and transport membranes. Among these many appealing applications, they have been studied in liquid-liquid extraction processes. The replacement of volatile solvents by ILs offers additional environmental advantages because of the low volatility of ILs and easiness of recycling, reducing therefore the solvents losses to atmosphere and aquatic streams. Several studies regarding ILs have already been published in the past few years in the recovery of acetone, antibiotics, ethanol and butanol from fermentation broths, and also on the removal of organic contaminants from aqueous waste streams [4-7]. Moreover, ILs were also investigated as solvents for multiphase biotransformation reactions [8].

One additional and vital feature of ILs is their character of “designer solvents”, since a large number of properties can be manipulated by the correct selection of the cation and/or anion [4, 9-11]. Moreover, the independent selection of both the cation and anion allows the fine-tunning of the ILs solvation/extraction performance which is an extremely important characteristic concerning biotechnological liquid-liquid separation processes. Nevertheless,

for the correct design and optimization of extraction processes making use of ILs, besides the biomolecules extraction investigations, a detailed understanding of ILs, water and inorganic salts or carbohydrates phase behaviour is of utmost importance.

Figure 2 shows the increased interest from scientists in the ILs topic over the recent years.

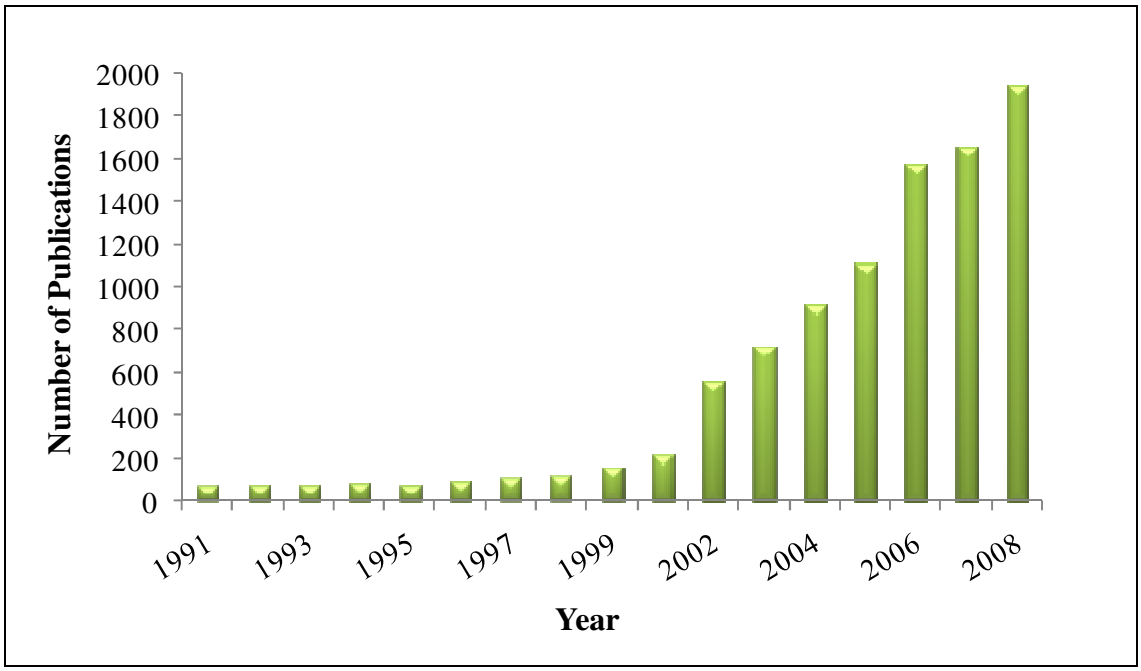

Figure 2 - Exponential growth of publications involving ionic liquids during 1991 to 2008 [12].

1.2. Extraction of Biomolecules using Aqueous Two-Phases Systems (ATPS)

Liquid–liquid extraction is a widely used separation process in analytical science and chemical industry. Generally, extraction with solvents makes use of the partitioning of a solute between two immiscible phases. The separation potential and feasibility of solvents for commercial, industrial or research applications depends thus on their physical properties such as boiling point, thermal stability, viscosity, ease of recovery, toxicity and corrosive nature of the solvent, as well as on the physical and chemical properties of the solute [13-18] .

The processes of fermentation face various limitations, some resulting from the accumulation of products in the bioreactor. The integration of fermentation bioprocesses with an initial step for the separation of the product can improve the product yield and facilitate the downstream processing. The liquid-liquid extraction seems to be the most promissing among the approaches that have been used for this purpose. Indeed, the extraction of metabolites produced *via* fermentation by liquid-liquid extraction has been the topic of many research activities and patents [1]. The efficiency of any fermentation process depends on downstream processing which ensures the purity and quality of the biomolecules. Since many biomolecules have narrow tolerance limits of pH, temperature, osmotic pressure, surface charges, among others, the extraction and isolation techniques should be specific and compatible to the product. Therefore, it is not surprising that about 60–90 % of the cost of a biological process is expended on downstream processing [19].

Aqueous two - phase systems (ATPS) provide an alternative and efficient approach for the purification of biomolecules by their partitioning between two liquid aqueous phases [19]. ATPS attracted augmented interest as a technique for the separation and purification of biomolecules such as proteins, enzymes and nucleic acids. There are three main typical kinds of ATPS: polymer + polymer, polymer + salt and salt + salt systems [14, 17, 18]. Recently, Gutowski et al. [20] have shown that imidazolium - based ILs are also able to form ATPS in the presence of inorganic salts, such as K_3PO_4. Above critical concentrations of the IL and inorganic salt in aqueous solution, phase separation takes place resulting in the formation of an IL - enriched upper and an inorganic salt - enriched lower phase. In those IL-based ATPS the major component in each of the two phases is

water, followed by IL and inorganic salt, thus providing an extraction technology that eliminates the need of VOCs [13]. In addition, IL-based ATPS offer the opportunity to combine the purification process of active biocatalysts with the enhanced performance of some enzymes in the presence of ionic media [1, 12, 21, 22]. Moreover, these new ATPS have many advantages afforded by the use of ILs, such as low viscosity, little emulsion formation, no need of using volatile organic solvent, quick phase separation, high extraction efficiency and gentle biocompatible environment. Furthermore, these new IL-based ATPS can be utilized to recycle or concentrate hydrophilic ILs from aqueous solutions.

Besides the interest on IL-based ATPS with inorganic salts, the application of carbohydrates to substitute those highly charged systems seems to be a more benign approach. The introduction of K_3PO_4 as salting-out inducing agent inevitably introduce potassium and phosphate ions, complicating the recycling process as hydrophilic ILs dissociate in aqueous solution. ATPS formed by the addition of carbohydrates [18, 23-25] seem to be a significant alternative to highly charged ATPS and particularly relevant in biochemical separations from fermentative medium, due to the availability of carbon and nitrogen - based nutrients for cells.

IL-based ATPS have been successfully used to separate testosterone, epitestosterone, opium alkaloids, bovine serum albumin and L-tryptophan [15, 16, 26]. Nevertheless, it is of main interest to obtain comparisons between solubilization and partition coefficients for other solutes and ILs, aiming at tailoring an “ideal” IL able for specific extractions, and to gain further insights on the molecular level mechanisms which control the solutes’ partitioning between different phases.

2. ILs + H_2O + K_3PO_4 Ternary Systems

2.1. General Context

Many metabolites and/or bioproducts present narrow tolerance limits of pH, ionic strength, osmotic pressure, surface charges and temperature; thus, the extraction and isolation techniques must be specific and compatible with the product. Conventional techniques used for product recovery from biotechnological processes are usually expensive and present low yields. There have been, therefore, considerable efforts from the industrial and academic communities for the development of cost - effective separation techniques, such as liquid - liquid extraction in ATPS [15].

In this work it was evaluated the ILs (phosphonium and choline-based salts) influence in promoting ATPS maintaining the same inorganic salt (K_3PO_4). Different phase diagrams (binodal curves and tie-lines) for different hydrophilic ILs + K_3PO_4 + water systems, at 298 K and atmospheric pressure, were determined. The binodal curves were fitted to a three-parameter equation and the tie-lines were estimated using the Merchuck et al. approach [27]. The selected ILs combination allowed the study of the cation nature and the anion identity impact in the ATPS promotion capability. In addition, the ATPS here investigated were characterized according to their extractive potential for biomolecules, where β-carotene, caffeine, rhodamine and L-tryptophan were selected as model biomolecules. Biomolecules are important compounds of several biotechnological processes and the development of methods for their separation and purification is still a main problem.

L-tryptophan, shown in Figure 3, is an aromatic amino acid containing an indole ring system. The aromatic side chains are relatively hydrophobic. L-tryptophan can thus participate in hydrophobic nature derived interactions, π···π type interactions, hydrogen-bonding, and electrostatic interactions at pH values different from the specific isoelectric point. L-tryptophan absorbs ultraviolet light resulting from the amino acid aromatic character. This accounts for the characteristic strong absorbance of light by most proteins at a wavelength of 280 nm, a property exploited by researchers in the characterization of proteins [28].

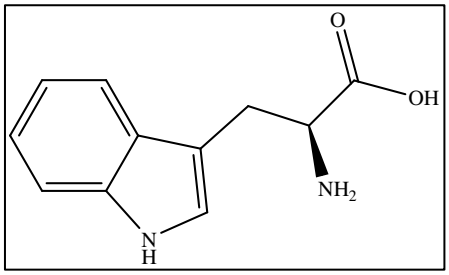

Figure 3 - Chemical structure of L-tryptophan.

β-carotene is a major product commonly used as provitamin A. It belongs to the polyene class of compounds, which accounts for its high reactivity as a free - radical inhibitor and antioxidant. β-carotene (Figure 4) readily undergoes isomerisation, particularly induced by oxygen on exposure to light and above 35 °C. Low-boiling solvents are usually used for β-carotene extraction from natural and synthetic sources, since they are easily removable from the extract under low pressure and readily recoverable [29]. Liquid - liquid extraction techniques are highly recommended as non-destructive methods and feasible at room temperature [29].

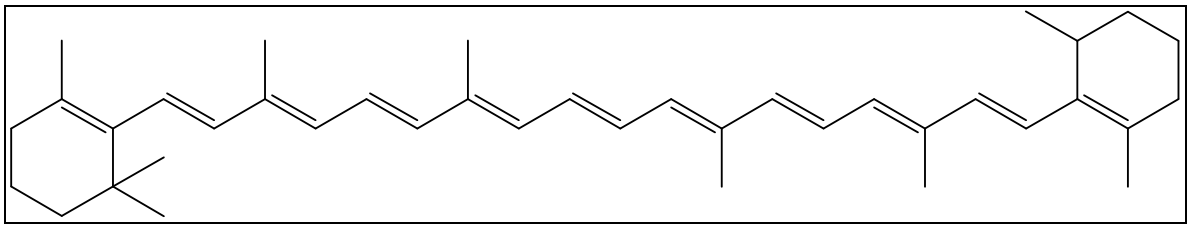

Figure 4 - Chemical structure of β-carotene.

Rhodamine (Figure 5) belongs to the family of fluorone dyes. Rhodamine derivatives are used as dyes and dye laser gain medium. It is often used as a tracer dye within water involving processes to determine the rate and direction of flow and transport. Rhodamine dyes are generally toxic, and highly soluble in water, methanol and ethanol [30].

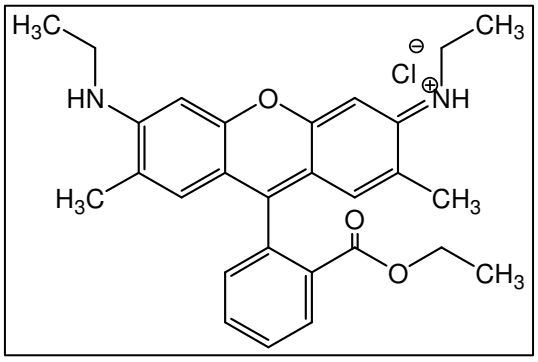

Figure 5 - Chemical structure of rhodamine 6G.

Caffeine (Figure 6) is usually referred to as a purine alkaloid [31]. Caffeine molecular structure is very closely linked with those of the purine bases such as adenine and guanine - fundamental components of nucleosides, nucleotides and nucleic acids. Caffeine is mainly present in beverages such as tea, coffee and cola and is one of the most widely consumed and socially accepted natural stimulants [32]. The solubility of caffeine in water is very small due to the alkaloid molecular structure which suffers self-association by hydrophobic nature derived

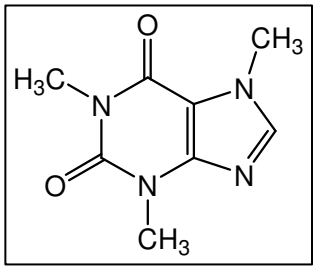

Figure 6 - Chemical structure of caffeine.

interactions. Caffeine also interacts and suffers complexation with several molecules of interest usually present in food and drug formulations [33].

ILs-based on the phosphonium cation usually contain four alkyl substituents (Figure **7**). The various combinations of possible cations along with the multitude of diverse anions represent an enormous number of combined salts. Not all phosphonium-based salts are liquid at room temperature; yet, by a judicious selection of the alkyl substituents as well as the appropriate anion, it is possible to obtain many phosphonium salts liquid at room temperature, and many more which fall within the broad general definition of ILs as salts with a melting point below 100 °C.

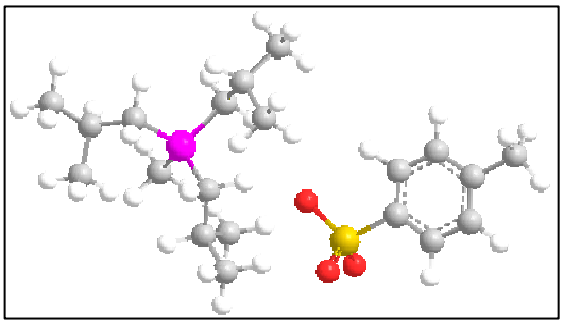

Figure 7 - Chemical structure of a common phosphonium-based IL (tri-isobutyl(methyl) tosylate).

Alkylphosphonium-based salts are, in general, less dense than water. This fact can be beneficial in product work-up steps towards decanting aqueous streams. Imidazolium-based salts, on the other hand, are usually denser than water [34, 35].

Most studies on ILs concern imidazolium salts, although pyridinium, pyrrolidinium, piperidinium, phosphonium, quaternary ammonium, and other organic salts are thoroughly being investigated as well [1, 34, 36] . ATPs employing imidazolium-based ILs are well known in literature [15, 17, 20]. Nevertheless, ATPS making use of phosphonium-based ILs were not explored until the present and will be presented here for the first time. A correct selection of hydrophilic phosphonium-based ILs in combination with a salting-out inducing inorganic salt (K_3PO_4) has shown to be able to form ATPS.

Choline chloride is a quaternary ammonium salt as shown in (Figure 8). Choline chloride (2-hydroxyethyltrimethylammonium chloride or vitamin B4) is a relatively cheap organic salt. Unfortunately, choline chloride has a high melting point (298 to 304 °C). Therefore, it is itself not an IL. Nevertheless, Abbott and co-workers obtained ILs by mixing choline chloride with hydrated

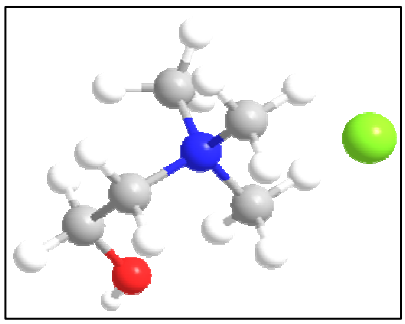

Figure 8 - Chemical structure of choline chloride

transition metal salts [37], or with anhydrous zinc(II) chloride or tin(II) chloride [38, 39]. The authors found [40] that choline chloride forms the so-called “deep eutectic solvents” with hydrogen bond donors; a mixture of urea and choline chloride in a 2:1 molar ratio is liquid at room temperature [41]. On the other hand, the melting points of ILs strongly depend on the nature of the anion [36]. Therefore it would be possible to obtain room-temperature choline-based ILs by replacing the chloride anions in choline chloride by other counterions [36, 40, 42]. Nonetheless, the application of the hydrophilic choline chloride with the inorganic salt K_3PO_4 leaded to liquid-liquid biphasic systems because this salt is highly miscible in aqueous phases.

2.2. Experimental Section

2.2.1. Chemicals

The ATPS studied in this work were established by using an aqueous solution of K_3PO_4 ≥ 98 wt % pure from Sigma and individual aqueous solutions of hydrophilic ILs. The ILs studied were choline chloride > 98 wt % pure from Sigma, and phosphonium-based ILs, namely triisobutyl(methyl)phosphonium tosylate (CYPHOS IL 106) > 95 wt % pure, tributyl(methyl)phosphonium methylsulphate (CYPHOS IL 108) > 98.6 wt % pure and tetrabutylphosphonium bromide (CYPHOS IL 163) > 96 wt % pure. The phosphonium-based ILs were kindly provided by Cytec Industries, Inc. All the ILs molecular structures are described in Figure 9.

For the validation of the experimental procedure it was used the 1-butyl-3-methylimidazolium chloride, [C_4mim][Cl] > 99 wt % pure from Iolitec. The biomolecules L-tryptophan > 99.0 wt % pure and β-carotene ≥ 97.0 wt % pure were obtained from Fluka, rhodamine 6G > 95.0 wt % pure for microscopy was acquired from Merck and caffeine ≥ 99.5 wt % pure, was obtained from José M. Vaz Pereira, SA. The water used was ultra-pure water, double distilled, passed by a reverse osmosis system and further treated with a Milli-Q plus 185 water purification apparatus.

Triisobutyl(methyl)phosphonium tosylate **(CYPHOS IL 106)**

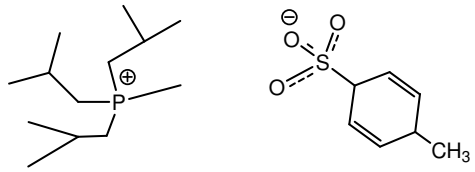

Tributyl(methyl)phosphonium methylsulfate **(CYPHOS IL 108)**

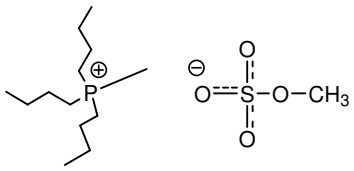

Tetrabutylphosphonium bromide **(CYPHOS IL 163)**

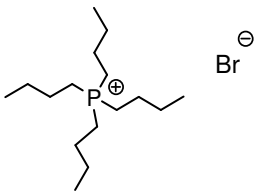

(2-Hydroxyethyl)trimethylammonium chloride **(Choline Chloride)**

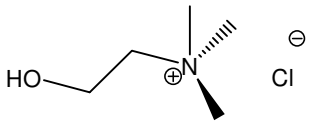

1-butyl-3-methylimidazolium chloride **([C_4mim][Cl])**

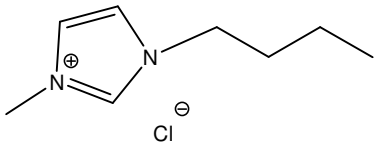

Figure 9 - Chemical structures of the studied ILs.

2.2.2. Experimental Procedure

2.2.2.1. Phase Diagrams

The phase diagrams were determined through the cloud point titration method at 298 K (± 1 K), as shown in Figure 10 [43, 44].

Aqueous solutions of K_3PO_4 at 40 wt % and aqueous solutions of the different hydrophilic ILs at variable concentrations were prepared and used for the phase diagrams determination. Repetitive drop-wise addition of the aqueous inorganic salt solution to the aqueous solution of IL was carried until the detection of a cloudy solution, followed by the drop-wise addition of ultra-pure water until the detection of a monophasic region (clear and limpid solution). Drop-wise additions were carried under constant steering. The ternary system compositions were determined by the weight quantification of all components added within an uncertainty of ± 10^{-4} g.

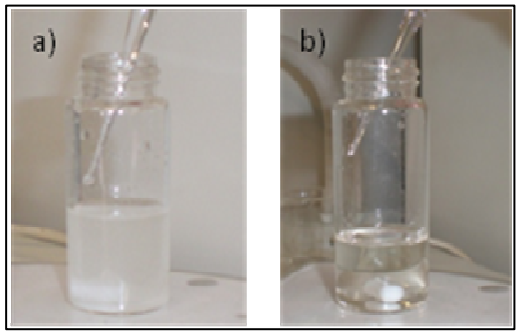

Figure 10 - Experimental determination of the binodal curve for the aqueous systems IL- K_3PO_4: a) addition of K_3PO_4 aqueous solution for the cloud point detection; b) addition of water for the clean point detection.

The experimental procedure adopted was validated with the phase diagram obtained for the [C_4mim][Cl] and K_3PO_4 aqueous system against literature data [1] . The comparison between the bimodal data obtained in this work and those reported in literature [45] is presented in Figure 11.

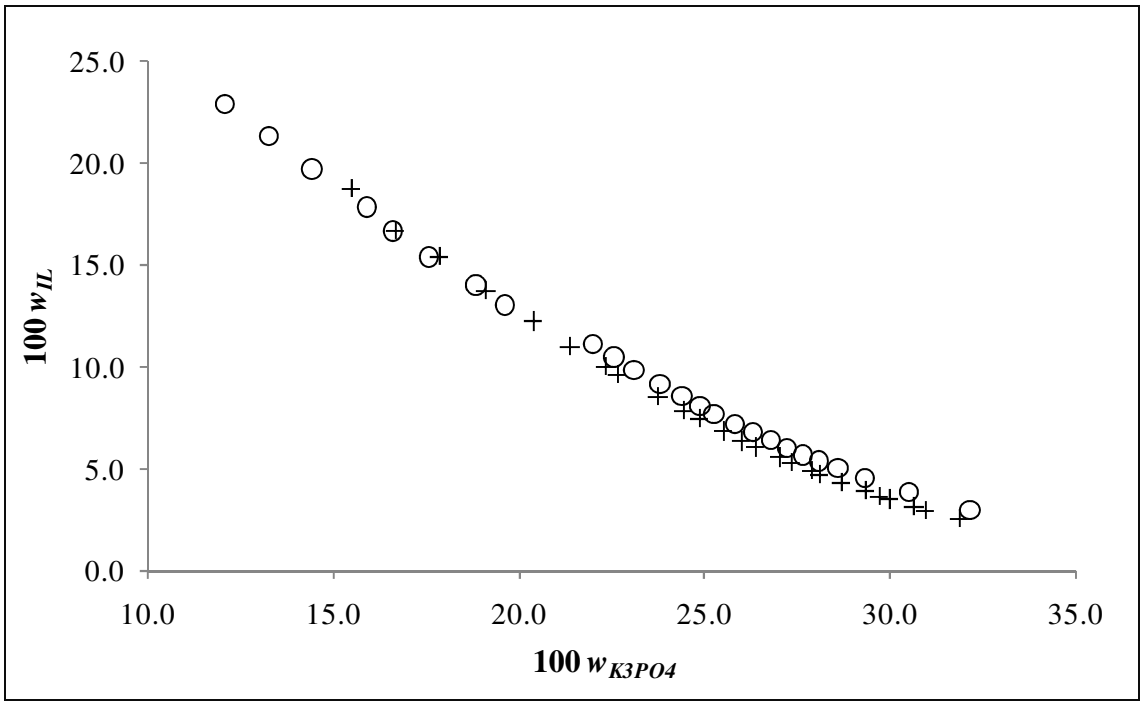

Figure 11 - Phase diagram for the ternary system composed by $[C_4mim][Cl]$ + K_3PO_4+ H_2O at 298 K: ○, this work; **+**, literature data [45].

2.2.2.2. Determination of Tie-Lines

The tie-lines (TLs) were determined by a gravimetric method described by Merchuck et al.[27]. For the TLs determination, a mixture at the biphasic region was prepared, vigorously agitated and allowed to reach the equilibrium by the separation of both phases for 24 h at 298 K using small ampoules (*ca*. 10 mL) especially designed for the purpose. After the separation step, both top and bottom phases were weighed. Each individual TL was determined by application of the lever rule to the relationship between the top mass phase composition and the overall system composition [27].

The experimental binodal curves were fitted using eq. 1 [27],

$$Y = A\exp\left[\left(BX^{0.5}\right) - \left(CX^{3}\right)\right] \quad (1)$$

where *Y* and *X,* are respectively, the IL and salt weight percentages, and *A*, *B* and *C* are constants obtained by the regression.

For the TLs determination it was solved the following system of four equations (eqs. 2 to 5) and four unknown values (Y_T, Y_B, X_T and X_B) [27]:

$$Y_T = A\exp\left[\left(BX_T^{0.5}\right) - \left(CX_T^{3}\right)\right] \quad (2)$$

$$Y_B = A\exp\left[\left(BX_B^{0.5}\right) - \left(CX_B^{3}\right)\right] \quad (3)$$

$$Y_T = \left(Y_M / \alpha\right) - \left(\left(1-\alpha\right)/\alpha\right)Y_B \quad (4)$$

$$X_T = \left(X_M / \alpha\right) - \left(\left(1-\alpha\right)/\alpha\right)X_B \quad (5)$$

where *M*, *T*, and *B* denote respectively the mixture, the top phase and the bottom phase, *X* is the weight fraction of inorganic salt, *Y* the weight fraction of IL and α is the ratio between the mass of the top phase and the total mass of the mixture.

The solution of the referred system gives the concentration of the IL and salt in the top and bottom phases, and thus the TLs can be easily represented.

For the calculation of the tie-lines length (TLL) it was used eq. 6 as follows,

$$TLL = \sqrt{\left(w_s^{\,top} - w_s^{\,bottom}\right)^2 - \left(w_{IL}^{\,top} - w_{IL}^{\,bottom}\right)^2} \quad (6)$$

where w_s and w_{IL} are the weight mass percentages of the salt and IL in the top or bottom phases.

2.2.2.3. Partitioning of Biomolecules

The partition coefficients of the studied biomolecules, K_{Trp} for L-tryptophan, $K_{\beta carot}$ for β-carotene, K_{Rhod} for rhodamine 6G and K_{Caf} for caffeine are defined as the ratio of the concentration of the biomolecule in the IL and in the K_3PO_4 aqueous-rich phases, and as described by eq. 7 (example for the L-tryptophan biomolecule),

$$K_{Trp} = \frac{[Trp]_{IL}}{[Trp]_{K3PO4}} \quad (7)$$

where $[Trp]_{IL}$ and $[Trp]_{K3PO4}$ are, respectively, the concentrations of L-tryptophan in the IL and in the K_3PO_4 aqueous -rich phases.

A mixture in the biphasic region was selected and used to evaluate the biomolecules partitioning. For this purpose aqueous solutions, with a concentration of approximately 0.78 $g \cdot dm^{-3}$ (3.8×10^{-3} $mol \cdot dm^{-3}$) for L-tryptophan, 0.15 $g \cdot dm^{-3}$ (0.28×10^{-3} $mol \cdot dm^{-3}$) for β-carotene, 0.015 $g \cdot dm^{-3}$ (0.031×10^{-3} $mol \cdot dm^{-3}$) for rhodamine 6G and 5.0 $g \cdot dm^{-3}$ (25×10^{-3} $mol.dm^{-3}$) for caffeine, were used. All biomolecules aqueous solutions can be considered at infinite dilution and completely solvated in aqueous media avoiding thus specific interactions between biomolecules. The biphasic solution was left to equilibrate for 12 h (a time period established in previous optimizing experiments) to achieve a complete biomolecule partitioning between the two phases. Due care was taken with β-carotene, which suffers isomerisation on exposure to light, maintaining the ampoules covered by aluminium paper during the time necessary for equilibration. The experimental procedure for each biomolecule extraction is depicted in Figure 12.

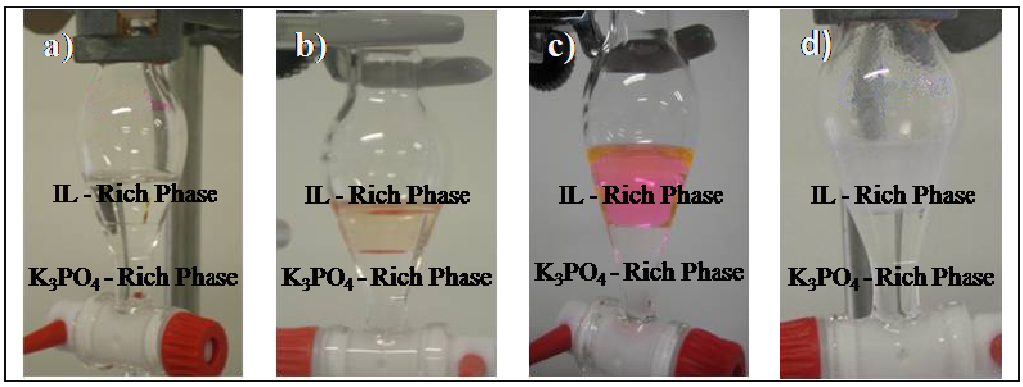

Figure 12 - Experimental procedure used for the determination of partition coefficients of L-tryptophan (a), β-carotene (b), rhodamine 6G (c) and caffeine (d).

The solute quantification, in both phases, was carried by UV-Vis spectroscopy using a SHIMADZU UV-1700, Pharma-Spec Spectrometer, at a wavelength of 279 nm, 512 nm, 527 nm and 234 nm respectively for L-tryptophan, β-carotene, rhodamine 6G and caffeine using calibration curves previously established (the calibration curves are presented in

Appendix A). All the wavelengths used for quantification of the biomolecules correspond to the maximum absorption peaks of each solute. Possible interferences of both the inorganic salt and the IL with the analytical method were taken into account and found to be of no significance at the dilutions carried. Two samples of each aqueous phase were precisely quantified and the standard deviations determined. Moreover, both phases were weighted and the corresponding TLs obtained as previously described.

2.3. Results and Discussion

2.3.1. Phase Diagrams and Tie-Lines

The solubility of a given solute in water is affected by the presence of an electrolyte. Moreover, the addition of an inorganic salt leads to a more complex phase equilibria than typical systems allowing, the appearance of different mechanisms, such as ion exchange and ion-pairing. Nevertheless, Bridges et al. [9] have shown that although ion partition can occur, the electroneutrality is maintained and that the overall deviations of the ions concentration at each TL are small enough and cannot be considered a significant source of error.

The experimental phase diagrams for IL + K_3PO_4 + H_2O systems at 298 K and atmospheric pressure are presented in Figure 13. All data are presented in molality units for a detailed understanding of the ILs impact on the ATPS formation (see experimental weight fraction data in Appendix B).

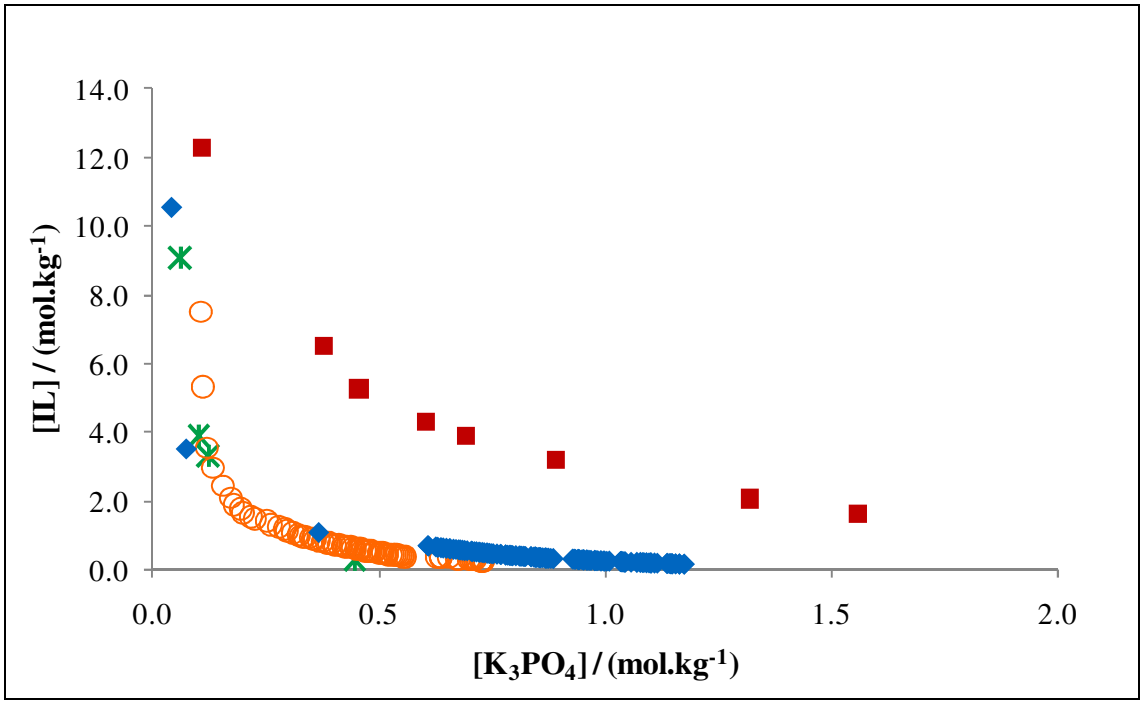

Figure 13 - Phase diagrams for phosphonium-based ILs and choline chloride ternary systems composed by IL + K_3PO_4 + H_2O at 298 K: ○, CYPHOS IL 106; ♦, CYPHOS IL 108; ✳, CYPHOS IL 163; ■, choline chloride.

Although there are several reports in literature describing imidazolium-based ILs and inorganic salts ATPS [15, 16, 20], this work is the first evidence that phosphonium and choline-based ILs also allow the phase separation process in aqueous systems. Considering the fixed distance between the binodal curves and the origin at 0.4 mol·kg^{-1} of K_3PO_4, the ability of phase formation is described by the following order: CYPHOS IL 163 < CYPHOS IL 106 < CYPHOS IL 108 < < choline chloride. This order shown that the more distant the origin is to the binodal curve, less salt is necessary to add at the aqueous system to promote the phase separation. Thus, choline chloride and CYPHOS IL 163 have, respectively, the lower and the higher ability to induce phase separation.

Accordingly to literature [9, 15], the ability of inorganic salts to promote the phase separation and, consequently, a salting-out effect follows the order: K_3PO_4 > K_2HPO_4 ≈ K_2CO_3 > KOH. Thus, anions with a higher valence (PO_4^{3-}) are better salting-out agents than those with a lower valence (OH^-) [15, 16]. Having in mind that PO_4^{3-} is a high charge density ion and taking into account Figure 13, it can be concluded that the farthest from the IL axis is located the binodal curve, the larger the IL anion salting-out inducing behaviour. Thus, choline chloride has the strongest salting-out inducing character, followed by the phosphonium-based ILs with methylsulfate, tosylate and bromide anions. On the other hand, the higher the water affinity of the IL (hydrophilic nature), the less effective it is on promoting ATPS. In this context, tetrabutylphosphonium bromide has shown to be the less hydrophilic IL in opposite to CYPHOS IL 106 and 108 that present, respectively, an aromatic character and a sulphate group at the anion. With respect to the choline chloride IL, the presence of a hydroxyl group allows the formation of hydrogen-bonds, which are responsible for the strong hydrophilic nature.

The experimental binodal data was fitted by least-squares regression using the well known approach of Merchuck et al. [27] (eq. 1). The correlation coefficients *A*, *B* and *C*, the corresponding standard deviations (σ) and the correlation coefficients (R^2) are given in Table 1.

Table 1 - Correlation parameters of eq.1 used to describe the binodal data.

IL + K_3PO_4 + Water systems	*A*	*B*	*C*	R^2	σ
CYPHOS IL 106	229.48	-0.8378	3.614×10^{-5}	0.9863	1.5682
CYPHOS IL 108	116.85	-0.5131	1.217×10^{-4}	0.9864	0.9612
CYPHOS IL 163	176.57	-0.7562	1.100×10^{-3}	0.9987	1.7838
Choline chloride	97.603	-0.2726	1.910×10^{-5}	0.9977	1.0719

It is observed that the empirical equation correctly fits the experimental data, as shown in Figure 14 and 15 for CYPHOS 106 + water + K_3PO_4 and choline chloride + water + K_3PO_4 systems, correspondingly (with the other systems presented in Appendix C). It is observed that the empirical equation is satisfactorily correlating the binodal curves of the investigated systems.

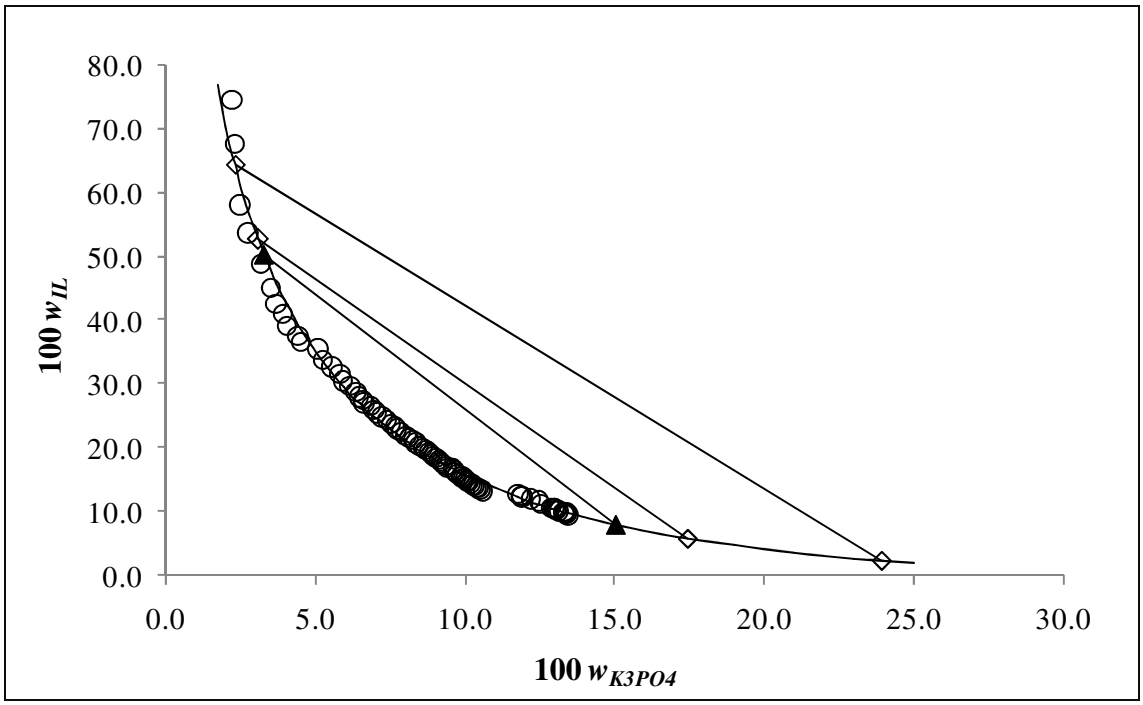

Figure 14 - Phase diagram for the ternary system CYPHOS 106 + K_3PO_4 + H_2O at 298 K:○, experimental binodal data; ◊, TL data; ▲, extraction TL data; ▬, binodal curve fit given by eq. 1**.**

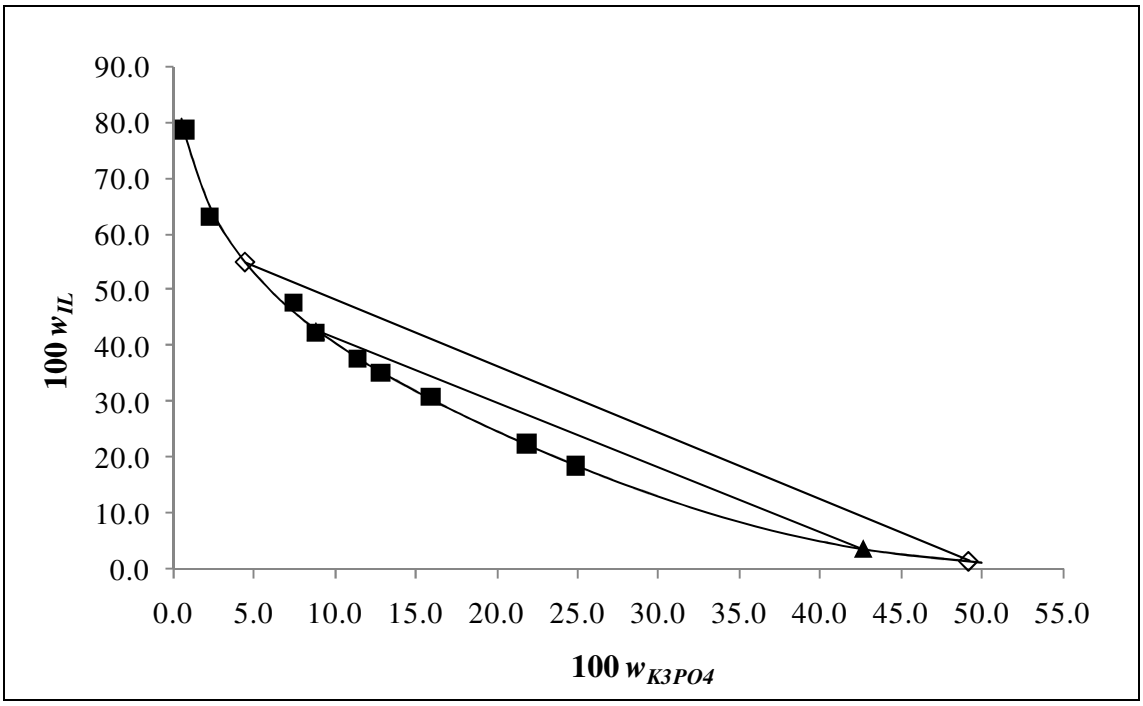

Figure 15 - Phase diagram for the ternary system choline chloride + K_3PO_4 + H_2O at 298 K: ■, experimental binodal data; ▲, extraction TL data; ◊, TL data; ▬, binodal curve fit given by eq. 1**.**

The tie-lines (TLs) of each ternary system were determined by a gravimetric method also described by Merchuck et al. [27], and previously described as eq. 2 to 5. The ternary weight fraction composition of the biphasic region used to calculate TL, TLs parameters and the respective TLLs, obtained by eq. 6, are reported in Table 2 and shown in Figure 14 and 15. Since the TLLs represent the difference between the IL and inorganic salt concentrations in the top and bottom phases, the higher the TLL, the higher is the IL composition in the top phase and the salt composition in the bottom phase.

Table 2 - Experimental data for TLs and TLLs at 298 K.

IL	Weight fraction composition (*wt*) %		TL equation[a]		TLL
	IL	K_3PO_4	*a*	*b*	
CYPHOS IL 106	39.71	10.90	71.07	-2.878	65.77
	30.07	9.980	62.76	-3.276	49.04
CYPHOS IL 108	22.98	9.986	48.60	-2.566	24.88
	20.13	15.11	57.16	-2.451	51.80
CYPHOS IL 163	40.98	5.930	71.70	-5.181	62.38
	49.95	6.516	79.54	-4.542	75.21
Choline chloride	29.91	20.07	53.08	-1.154	51.95
	29.80	25.47	60.22	-1.194	69.72

[a] $IL\ (wt\ \%) = a + b \cdot K_3PO_4\ (wt\ \%)$

2.3.2. Partitioning of Biomolecules

Biomolecules, such as proteins and enzymes, are usually produced at industrial scale using enzymatic or fermentation processes. Separation and purification steps are difficult and really expensive. Since high purity is needed for biomolecules' applications, the use of ATPS is of great importance. The success of the extractive potential of ATPS depends largely on the ability to manipulate phase properties in order to obtain the appropriate partition coefficients and selectivity for the biomolecule of interest. There are several approaches to manipulate a particular solute partitioning, such as the application of different salts and/or ILs or changing either the concentration of salt and IL (control of the solute's affinity) and the introduction of additional co-solvents, anti-solvents or amphiphilic structures (control of the overall system).

The salt and IL compositions selected for the biomolecule partitioning, as well the respective partition coefficients, TLs and TLLs obtained in this work, are reported in Table 3. Figure 16 presents the general comparison among the diverse solutes partitioning coefficients. From the results it can be established that the addition of biomolecules in the water phase, at least at low enough concentrations, has no influence in the TLs and TLLs, previously described (Figures 14 and 15). Indeed, these TLs and TLLs can be considered

additional phase equilibrium TLs for each individual ATPS. This fact was previously observed [46] and is in close agreement with the results obtained in this work.

Table 3 - Weight fraction composition and partition coefficients of L-tryptophan, β-carotene, rhodamine 6G and caffeine in ILs - ATPS systems at 298 K.

IL	*Mr*	Weight fraction composition (*wt %*)		TL equation[a]		TLL	$K_i \pm \sigma$
		IL	K_3PO_4	*a*	*b*		
L-tryptophan							
CYPHOS IL 108	328.45	22.95	10.66	50.39	-2.574	31.86	9.0 ± 0.1
Choline chloride	139.63	29.91	19.99	38.31	-0.8940	51.58	25.7 ± 0.2
β-carotene							
CYPHOS IL 106	388.55	39.62	6.516	64.22	-3.776	46.04	61.75
Choline chloride	139.63	29.95	20.10	53.13	-1.154	52.20	2.1 ± 0.1
rhodamine 6G							
CYPHOS IL 106	388.55	40.11	6.118	62.23	-3.615	44.14	3.6 ± 0.1
CYPHOS IL 108	328.45	23.66	10.22	48.61	-2.442	29.94	8 ± 1
CYPHOS IL 163	339.34	39.92	5.995	72.86	-5.494	62.73	0.018 ± 0.007
Choline chloride	139.63	29.90	19.99	53.01	-1.156	51.52	13.4 ± 0.6
caffeine							
CYPHOS IL 108	328.45	23.62	10.26	49.49	-2.521	30.38	4.75 ± 0.01
Choline chloride	139.63	30.25	19.84	52.36	-1.114	52.57	108 ± 7

[a] IL (*wt %*) = $a + b \cdot K_3PO_4$ (*wt %*)

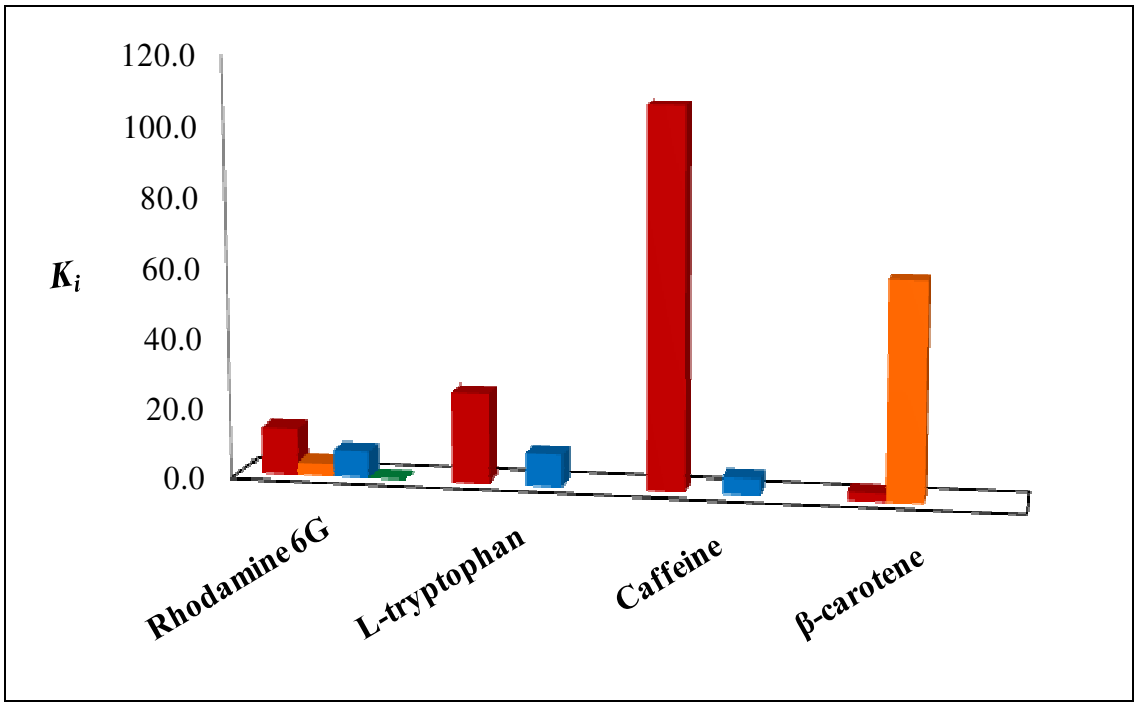

Figure 16 - Partitioning coefficients for each biomolecule (K_i) in different ILs + K_3PO_4 + water systems at 298 K: ■, CYPHOS IL 106; ■, CYPHOS IL 108; ■, CYPHOS IL 163; ■, Choline chloride.

During the partitioning of L-tryptophan, rhodamine 6G, β-carotene and caffeine there are several competing interactions between the IL, the inorganic salt, the biomolecules and water. Hydrogen-bonding, π···π interactions, hydrophobic nature derived interactions as well as electrostatic interactions between different compounds, are examples of these interactions. L-tryptophan, rhodamine 6G and caffeine here reported, are considered as quite hydrophilic biomolecules. In general, the results indicate that the K_i of the three biomolecules mentioned above, increases with the IL hydrophilic nature, being choline chloride the most efficient in their extraction. On the other hand and, since the β-carotene is highly hydrophobic with negligible solubility in water, its extraction is more efficient with CYPHOS IL 106, a phosphonium-based IL with low affinity for water.

Besides the hydrophilic/hydrophobic nature of ILs, the presence of an inorganic salt also leads to the biomolecules salting-out from the aqueous phase, further enhancing the distribution ratio of each biomolecule. However, the effect of the IL on the extraction ability of these systems can be gauged from the results of Salabat et al.[47], where a conventional PEG-based ABS was used for L-tryptophan extraction with much lower

partition coefficients (K_{Trp} ≈ 1 to 7) than the obtained in this work, for the same biomolecule (K_{Trp}= 9.0 and 25.7 for CYPHOS IL 108 and choline chloride, respectively). Nevertheless, no partition coefficients regarding the remaining solutes here described were found in literature which implies that no comparisons can be made. Yet, it can be established that the high K_i obtained with IL-based ATPS for the extraction of biomolecules show that these systems may be a successful and a clean approach for biomolecules separation and purification in biotechnological processes. Moreover, the large range obtained in the partition coefficients by changing the IL, indicates that the individual biomolecules extraction efficiency can be manipulated by the correct choice of the IL cation and/or anion.

2.4. Conclusions

The ability of hydrophilic ILs to form salt–salt ATPS allows them to be used in aqueous separation systems, opening the door to multiple applications (e.g., metathesis, separation of biological species or inorganics). For the first time, it was shown that phosphonium and choline-based ILs are also able to suffer salting-out in the presence of the inorganic salt K_3PO_4. The novel phase diagrams for the ternary systems composed by IL + water + K_3PO_4, at 298 K and atmospheric pressure, were determined and presented. The capacity of IL-based ATPS as prospective extraction media in biotechnological processes was demonstrated by the high partition coefficients obtained for several biomolecules ranging from amino acids to colorant dyes and alkaloids. In addition, it was demonstrated that the partition coefficients of biomolecules can be manipulated by the correct adjustment and combination of IL cation and anion.

3. ILs + H_2O + Carbohydrates Ternary Systems

3.1. Introduction

In recent years there has been a growing interest on the applications of ILs in liquid-liquid extraction of metal ions and organic compounds [48].

The 1-*n*-butyl-3-methylimidazolium hexafluorophosphate, [C_4mim][PF_6] (Figure 1), was used by Rogers and co-workers in the pioneer works using ILs for the liquid-liquid extraction of organic compounds from aqueous solutions [48]. Nevertheless, these type of studies mainly focus on hydrophobic ILs that form a biphasic solution in the presence of water (at room temperature and atmospheric pressure). Indeed, an increasing number of publications describing the use of ILs with low solubility in water as biphasic extraction media have been published in the past few years [4, 5, 49]. Nevertheless, from recent works it is becoming clear that hydrophilic ILs and thus ILs-based ATPS present higher efficiency in the recovery of biomolecules [17, 50].

Most of the systems reported [17, 20, 45], as well as the ternary systems presented before in this thesis, concern high concentrations of inorganic salts to induce IL-based ATPS. Nonetheless, recent works demonstrate that the hydrophilic IL (and thus miscible with water) 1-butyl-3-methylimidazolium tetrafluoroborate, [C_4mim][BF_4], can be induced to form ATPS when contacted with concentrated solutions of sugars (namely, sucrose, glucose, xylose and fructose), forming an upper IL-rich phase and a lower sugar-rich phase [13, 23-25]. These proposed systems are more environmentally benign than typical IL/inorganic salt systems, since the latter inevitably introduce potassium and phosphate ions, complicating the recycling process [23]. On the other hand, the presence of carbohydrates in a fermentation broth can be used both as salting-out agents as well as a carbon source to cells.

Carbohydrates are often classified according to the number of saccharide units they contain. A monosaccharide is a simple carbohydrate (single aldose and ketoses) that not hydrolyse to simpler sugars. The aldohexose D-Glucose, ($C_6H_{12}O_6$), for example, is a monosaccharide. On the other hand, a disaccharide when hydrolyzed is cleaved into two monosaccharides, which may be the same unit or different units of monosaccharides. For example, sucrose is a disaccharide that yields one molecule of glucose and one of fructose on hydrolysis, what can be described by the following scheme,

$$\text{Sucrose } (C_{12}H_{22}O_{11}) + H_2O \longrightarrow \text{Glucose } (C_6H_{12}O_6) + \text{Fructose } (C_6H_{12}O_6)$$

Polysaccharides are hydrolysed to more than 10 monosaccharide units. Some examples of saccharides (and the ones studied in this thesis) are depicted in Figure 17.

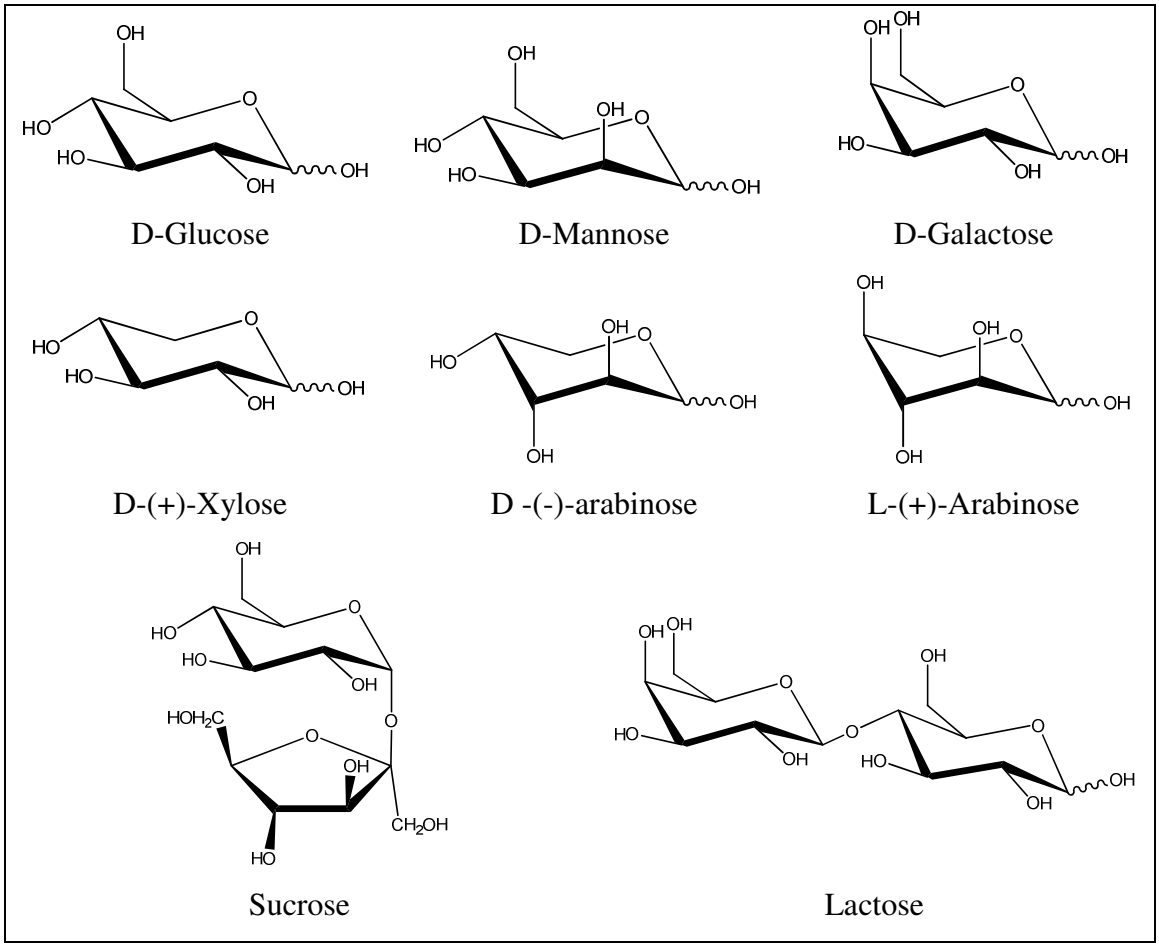

Figure 17 - Chemical structures of the studied saccharides.

Because the cyclic and linear forms of aldoses and ketoses do interconvert, these sugars undergo reactions that are typical of aldehydes and ketones. Aldoses and ketoses can be reduced to an alcohol function. Typical procedures include catalytic hydrogenation and sodium borohydride mediated reduction as shown in the following scheme.

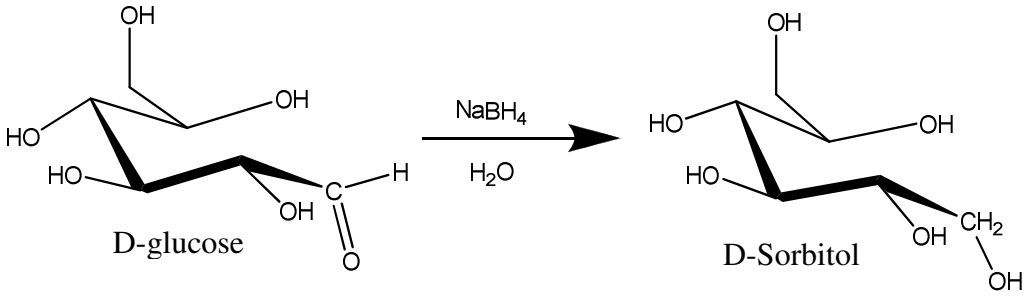

The products of carbohydrates reduction are called alditols. Since these alditols lack a carbonyl group, they are incapable of forming cyclic hemiacetals and exist exclusively in noncyclic forms. For example, reduction of D-glucose yields sorbitol and reduction of xylose yields xylitol, while reduction of D-fructose yields a mixture of glucitol and mannitol, corresponding to the two possible configurations at newly generated steregenic at C-2. Moreover, maltitol is a disaccharide obtained by hydrogenation of maltose. Figure 18 presents some examples of the chemical structures of alditols and studied in this thesis.

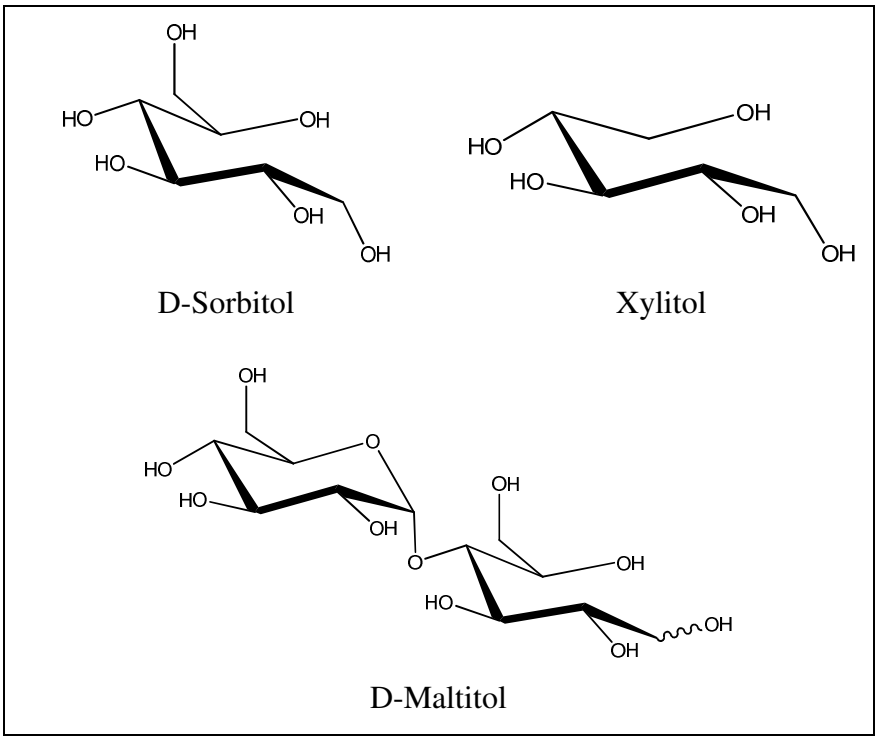

Figure 18 - Chemical structures of the studied alditols.

Aiming at gathering further information on the carbohydrates ability to induce ATPS with hydrophilic IL, in this work it was evaluated both the ILs and carbohydrates influence on promoting ATPS. Different phase diagrams (binodal curves and tie-lines) for systems of hydrophilic ILs + water + carbohydrates, at 298 K and atmospheric pressure, were determined. The binodal curves were fitted to a three-parameter equation and the TLs were estimated using the Merchuck et al. [27] approach as described before.

Besides the ATPS shown in literature regarding carbohydrates and $[C_4mim][BF_4]$ [13, 23-25], it is here demonstrated that further saccharides, as well as alditols, are able to induce phase separation of ILs aqueous solutions. In addition, the ATPS here investigated were

characterized according to their extractive potential for aminoacids, where L-tryptophan (Figure 3) was selected as a model biomolecule. Aminoacids are important compounds of several biotechnological processes and the development of methods for their separation and purification is still a problem.

3.2. Experimental Section

3.2.1. Chemicals

The ATPS studied in this work were established by using different aqueous solutions of carbohydrates and several aqueous solutions of hydrophilic ILs. The carbohydrates studied were: D-sorbitol≥ 98.0 wt % pure from Fluka, xylitol ≥ 99.0 wt % pure and maltitol ≥ 98.0 wt % pure both from Sigma, D-glucose ≥ 99.0 wt % pure and D-(+)-mannose ≥ 99.0 wt % pure both from Fluka, sucrose ≥ 99.5 wt % pure from Himedia, D-(+)-galactose≥ 98.0 wt % pure from GPR Rectapur, D-(+)-xylose ≥ 99.0 wt % pure from Carlo Erba, L-(+)-arabinose ≥ 99.0 wt % pure from BHD Biochemicals and D-(-)-arabinose ≥ 99.5 wt % pure from Sigma. The ILs studied were 1-butyl-3-methylimidazolium tetrafluoroborate, $[C_4mim][BF_4]$, 1-butyl-3-methylimidazolium chloride, $[C_4mim]Cl$, 1-hexyl-3-methylimidazolium chloride, $[C_6mim]Cl$, 1-benzyl-3-methylimidazolium chloride, $[C_7H_7mim]Cl$, 1-ethyl-3-methylimidazolium methylsulfate, $[C_2mim][MeSO_4]$, 1-butyl-3-methylimidazolium dicyanamide, $[C_4mim][N(CN)_2]$, 1-butyl-3-methylimidazolium hydrogenosulfate, $[C_4mim][HSO_4]$ and 1-butyl-3-methyl-imidazolium trifluoromethanesulfonate, $[C_4mim][CF_3SO_3]$. All the ILs were acquired at Iolitec and are ≥ 99.0 wt % pure. The purity of the ILs was confirmed by ^{1}H, ^{13}C and ^{19}F NMR spectra, being the ILs molecular structures described in Figure 9.

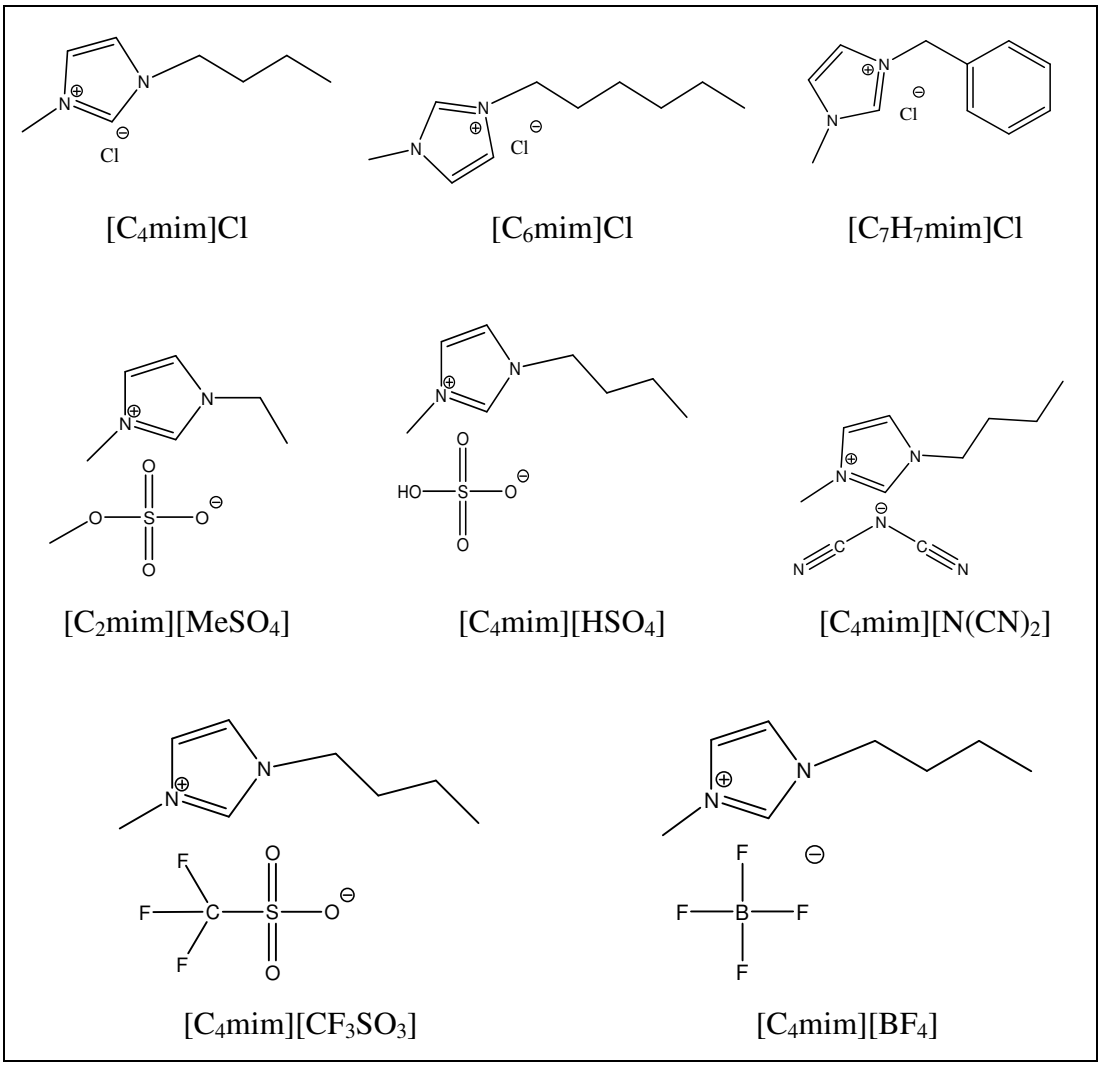

Figure 19 - Chemical structure of the studied ILs.

The water used was ultra-pure water, double distilled, passed by a reverse osmosis system and further treated with a Milli-Q plus 185 water purification apparatus. The L-tryptophan with a purity > 99.0 w/w % was from Fluka.

3.2.2. Experimental Procedure

The experimental procedure adopted was similar to the one described in Section 2.3. of this thesis. Instead of K_3PO_4 aqueous solutions several aqueous solutions of carbohydrates were employed. Aqueous solutions of each carbohydrate at 22-60 wt % (depending on each carbohydrate saturation solubility in water) and aqueous solutions of the different hydrophilic ILs at variable concentrations were prepared and used for the phase diagrams determination. Repetitive drop-wise addition of the aqueous carbohydrate solution to the aqueous solution of IL was carried until the detection of a cloudy solution, followed by the drop-wise addition of ultra-pure water until the detection of a monophasic region and limpid solution. Drop-wise additions were carried under constant steering. The ternary system compositions were determined by the weight quantification of all components added within an uncertainty of $\pm 10^{-4}$ g.

The experimental procedure adopted was validated with the phase diagram obtained for $[C_4mim][BF_4]$ + D-glucose + water ternary system at 298 K against literature data [23] and shown in Figure 20.

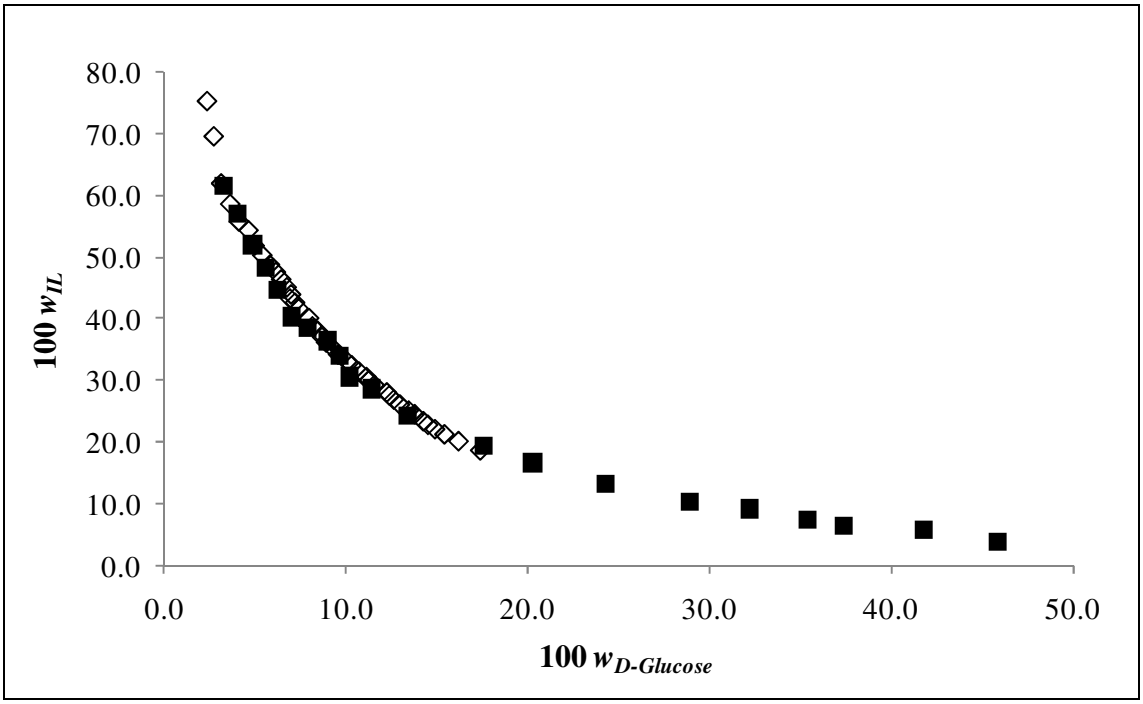

Figure 20 - Phase diagram for ternary systems composed by $[C_4mim][BF_4]$ + D-glucose + IL + H_2O at 298 K: ◊, this work; ■, literature data [23].

The TLs and TLLs were determined by a gravimetric method described by Merchuck et al. [27] and presented in Section 2.3.

The partition coefficients of L-tryptophan, K_{Trp}, are defined as the ratio of the concentration of the L-tryptophan in the IL and in the carbohydrate aqueous-rich phases, and as described by eq. 8,

$$K_{Trp} = \frac{[Trp]_{IL}}{[Trp]_{CH}} \quad (8)$$

where $[Trp]_{IL}$ and $[Trp]_{CH}$ are the concentration of L-tryptophan in the IL and in the carbohydrate aqueous-rich phases, respectively.

A mixture in the biphasic region was selected and used to evaluate the L-tryptophan partitioning. For this purpose aqueous solutions of L-tryptophan with a concentration of approximately 0.78 $g \cdot dm^{-3}$ (3.8×10^{-3} $mol \cdot dm^{-3}$) were used. The biphasic solution was left to equilibrate for 12 h and the aminoacid quantification, in both phases, was carried by UV spectroscopy using a SHIMADZU UV-1700, Pharma-Spec Spectrometer, at a wavelength of 279 nm and using calibration curves previously established (see Appendix A). Moreover, both phases were weighted and the corresponding TLs obtained as previously described.

3.3. Results and Discussion

3.3.1. Phase Diagrams and Tie-Lines

The ILs studied in this work were [C_4mim]Cl, [C_6mim]Cl, [C_7H_7mim]Cl, [C_2mim][$MeSO_4$], [C_4mim][$N(CN)_2$] and [C_4mim][HSO_4]. Although all the ILs mentioned were tested with sucrose aqueous solutions to infer about their ability to induce ATPS, only [C_4mim][BF_4] and [C_4mim][CF_3SO_3] were shown to undergo phase separation. This phenomenon can be explained by the ILs hydrophilic nature and/or affinity for water. As previously reported, the ability of imidazolium-based ILs for aqueous phase separation was shown to closely follow the hydrogen bond accepting strength decrease of the anions composing the IL [51]. Only fluoride-based and ILs with less affinity for water were able to promote the phase separation in the presence of carbohydrates. Nevertheless, these results confirm the ILs character of "designer solvents", and a large number of properties can be manipulated by the correct selection of the IL cation and/or anion.

In this work, it was investigated the phase diagrams of [C_4mim][CF_3SO_3] + carbohydrates + water, at 298 K and atmospheric pressure, in order to infer on the carbohydrate potential to induce ATPS. The binodal curves for each IL + carbohydrate + H_2O system are presented in Figure 21. That binodal data are listed in molality units for a detailed understanding of the carbohydrate impact on the ATPS formation (see Appendix D with the experimental weight fraction data: Table D 2, Table D 3, Table D 4).

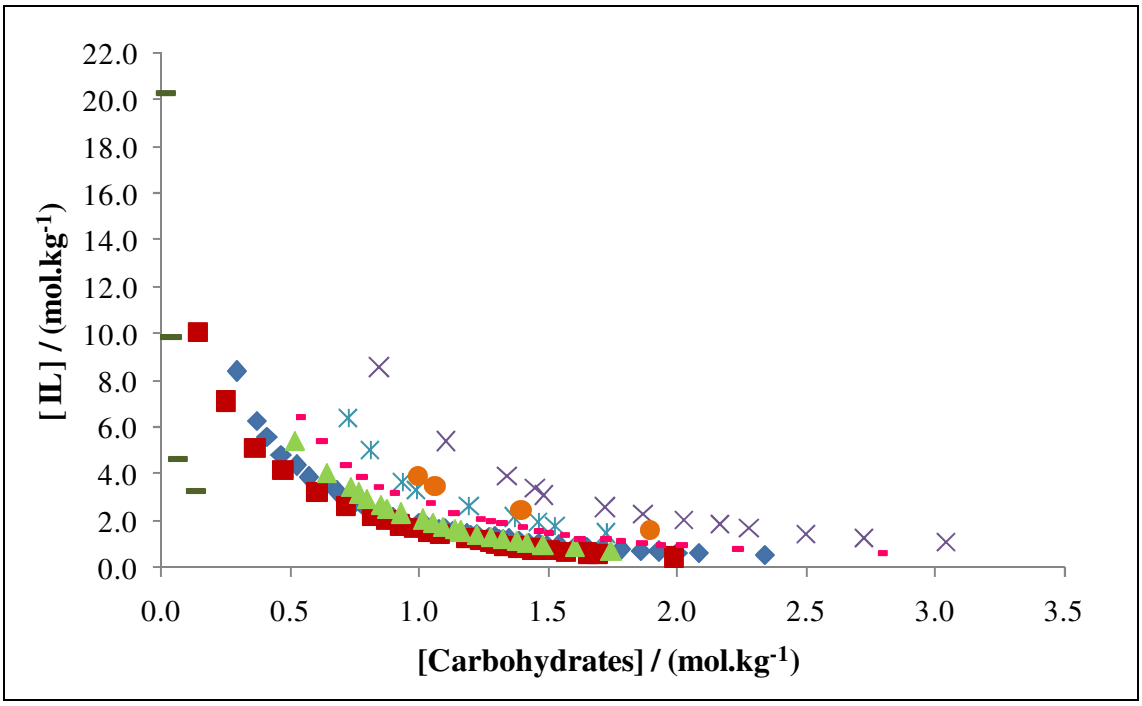

Figure 21 - Phase diagrams for ternary systems composed by $[C_4mim][CF_3SO_3]$ + carbohydrates + H_2O at 298 K: ♦, D-glucose; ■, sucrose; ▬, lactose; ×, D-(+)-xylose; ●, L-(+)-arabinose; ▲, D-(+)-galactose; ‾, D-(+)-mannose, ✳, D-(-)-arabinose.

Phase diagrams shown in Figure 21 indicate that the distance between binodal curves and the origin is in the increasing order: lactose < sucrose < D-glucose < D-(+)-galactose < D-(+)-mannose < D-(-)-arabinose < L-(+)arabinose < D-(+)-xylose.

The phase diagrams determined at 298 K and at atmospheric pressure, for each alditol + $[C_4mim][CF_3SO_3]$ + H_2O systems are presented in Figure 22, again in molality units for a detailed understanding of the alditol impact on the ATPS formation (see Appendix D with the experimental weight fraction data: Table D 5, Table D 6).

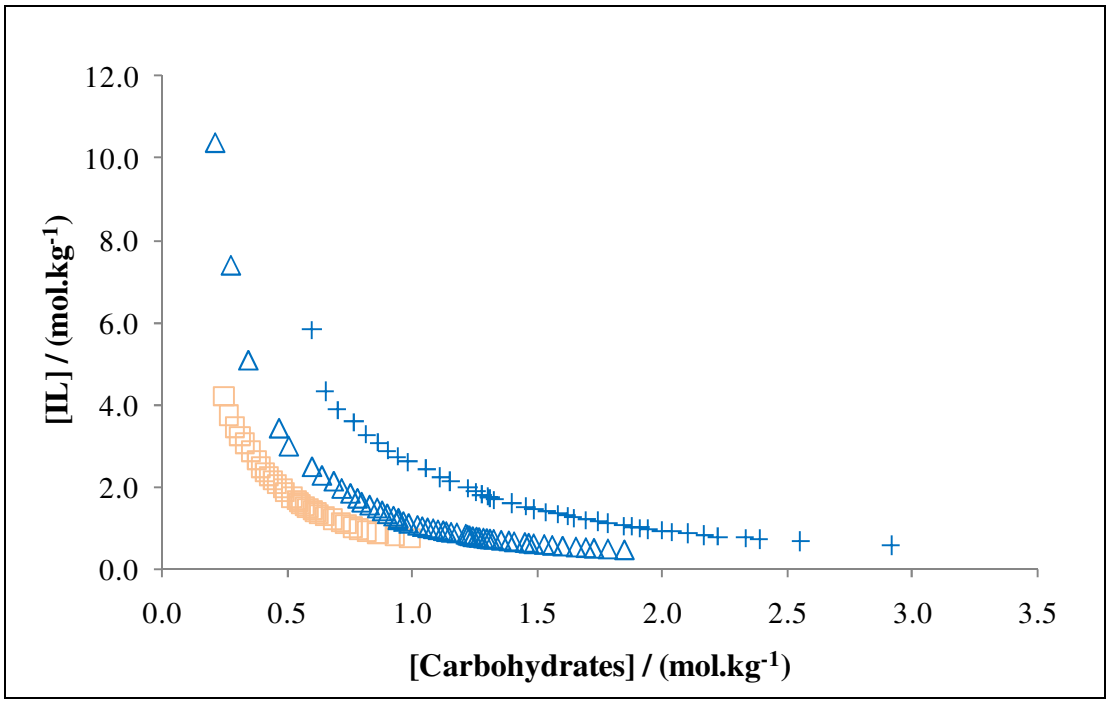

Figure 22 - Phase diagrams for ternary systems composed by $[C_4mim][CF_3SO_3]$ + alditols + H_2O at 298 K: Δ, D-sorbitol; □, maltitol; +, xylitol.

Figure 22 shows that the sequence on forming ATPS for alditols follows the order: maltitol > D-sorbitol > xylitol, implying that less carbohydrate is needed to form ATPS with $[C_4mim][CF_3SO_3]$. Finally, Figure 23 shows the set of all systems previously described for carbohydrates.

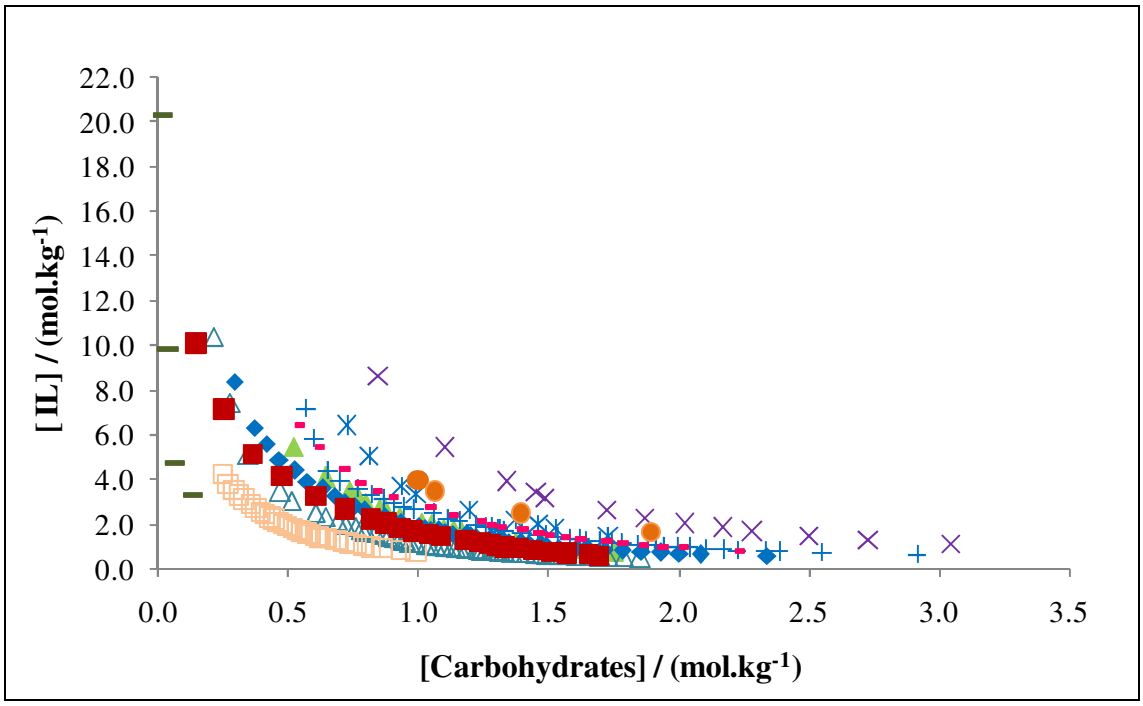

Figure 23 - Phase diagrams for ternary systems composed by $[C_4mim][CF_3SO_3]$ + carbohydrates + H_2O at 298 K: +, xylitol; □, maltitol; Δ, D-sorbitol; ×, D-(+)-xylose; —, lactose; ■, sucrose; ●, L-(+)-arabinose; ▲, D-(+)-galactose; ✳, D-(-)-arabinose; ¯, D-(+)-mannose; ♦,D-glucose.

Figure 23 shows that the distance between binodal curves and the origin is in the increasing order: lactose < maltitol < sucrose ≈ D-sorbitol < D-glucose < D-(+)-galactose < D-(+)-mannose ≈ xylitol < D-(-)-arabinose < L-(+)-arabinose < D-(+)-xylose. These results can be explained by two different factors such as the presence of -OH groups on ring sugar molecules and their stereochemistry. These factors make them salting-out agents. Galema and co-workers[52] concluded that the hydration of saccharides depends mainly on the relative position of the OH-4 group with respect to the nearest neighbor (the OH-2 group) in the pyranose ring. The conformations with an axial OH-4 and equatorial OH-2 are the least compatible with the three-dimensional hydrogen bonded structure of water, which means the dominant conformers of D-glucose. We can see that lactose, maltitol and sucrose have more -OH groups than D-sorbitol, and this latest sugar presents more -OH groups than the isomers D-glucose, D-(+)-mannose and D-(+)-galactose. The ability of xylitol to induce the phase separation is similar to the ability of the isomers mentioned above, since the number of -OH groups is the same. Moreover it was shown that conformational isomerism of monosaccharides present some impact through ATPS

formation where L-(+)-arabinose has shown to be more efficient than D-(+)-arabinose in supporting the [C_4mim][CF_3SO_3] salting-out.

The experimental binodal data of D-glucose, D-(+)-mannose, D-(+)-xylose and sucrose was fitted by least- squares regression through eq. 1 [27] being the correlation coefficients *A*, *B* and *C*, the corresponding standard deviations (σ) and the correlation coefficients (R^2) given in Table 4. Because the solubilisation of the remaining carbohydrates in water proved to be extremely low, the determination of TL, TLLs and of the partitioning coefficients of L-tryptophan was not carried.

Table 4 - Correlation parameters of eq. 1 used to describe the binodal curves.

IL + CH + Water system	*A*	*B*	*C*	R^2	σ
Sucrose	109.225	-0.1723	2.1876×10^{-5}	0.9995	0.4194
D-glucose	165.918	-0.3711	2.7861×10^{-5}	0.9977	0.7195
D-(+)-mannose	179.748	-0.3402	2.2041×10^{-5}	0.9976	0.6981
D-(+)-galactose	202.243	-0.3971	4.0411×10^{-5}	0.9982	0.5282
D-(+)-xylose	264.058	-0.3851	9.5264×10^{-6}	0.9991	0.4641
D-(-)-arabinose	351.946	-0.5432	4.8687×10^{-14}	0,9964	0,8304
L-(+)-arabinose	217.468	-0.3862	1.1199×10^{-5}	0.9977	0.8064
Lactose	125.468	-0.4627	2.0876×10^{-11}	0.9590	5.7513
Maltitol	168.898	-0.3961	2.0004×10^{-5}	0.9983	0.4452
D-sorbitol	206.444	-0.5096	2.6439×10^{-5}	0.8920	0.9958
Xylitol	231.366	-0.4624	1.0995×10^{-5}	0.9967	0.7043

As shown in Figure 24, it was observed that the Merchuck [27] approach (eq. 1) reasonable fits the experimental binodal data here reported, where the experimental data presented for the remaining carbohydrates in presented in Appendix E.

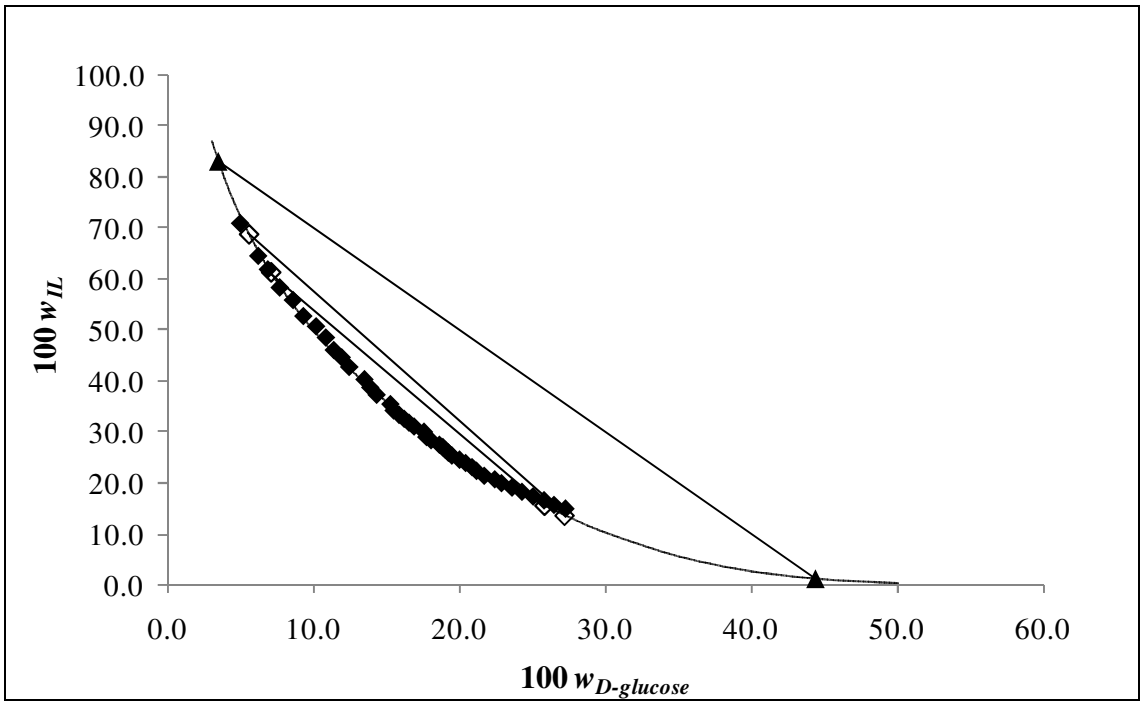

Figure 24 - Phase diagram for the ternary system composed by D-glucose + $[C_4mim][CF_3SO_3]$ + H_2O at 298 K: ♦, experimental binodal data; ◊, TL data; ▲, extraction TL data; ▬, fitting of experimental data by eq. 1**.**

The TLs and TLLs presented in Table 5 were determined by the gravimetric method of Merchuck et al. [27], using eqs. 2 to 6 presented before.

Table 5 - Experimental data for the tie lines (TLs) and tie line length (TLL) for the $[C_4mim][CF_3SO_3]$ + carbohydrates + water systems, at 298 K.

Carbohydrates	Weight fraction composition (*wt %*)		TL equation[a]		TLL
	IL	CH	*a*	*b*	
Sucrose	35.05	29.98	75.07	-1.335	75.72
	44.71	29.76	91.34	-1.567	105.3
D-glucose	37.90	16.67	78.47	-2.434	49.46
	29.29	21.09	82.96	-2.544	59.34
D-(+)-galactose	39.96	17.01	88.83	-2.874	58.87
	35.05	16.98	85.07	-2.945	37.53
D-(+)-mannose	39.92	20.14	85.29	-2.253	59.50
	43.46	21.23	87.31	-2.066	75.32
D-(+)-xylose	52.11	21.18	94.58	-2.006	68.52
	42.73	22.82	90.67	-2.100	47.21
L-(+)-arabinose	39.95	20.13	81.93	-2.086	43.08
	49.81	19.97	87.72	-1.898	73.37
D-(-)-arabinose	---[b]	---[b]	---[b]	---[b]	---[b]
Lactose	---[b]	---[b]	---[b]	---[b]	---[b]
Maltitol	49.92	20.08	106.3	-2.807	101.1
	34.88	20.05	82.01	-2.350	64.84
D-sorbitol	39.76	14.93	82.72	-2.876	62.59
	41.61	12.89	80.51	-3.017	53.48
Xylitol	34.97	20.19	79.48	-2.204	52.33
	30.07	20.04	77.80	-2.382	37.55

[a] IL (*wt %*) = $a + b \cdot$CH (*wt %*)

[b] not experimentally determined

For shorter TLLs, the TLs are approximately parallel, while for longer TLLs the tie-lines slopes start to deviate. These deviations are in agreement with some literature reports [53], and are related with the almost absence of IL on the carbohydrate-rich phase.

3.3.2. Partitioning of L-tryptophan

Taking in account that the main idea of the present work is the development of methods for the separation and purification of biomolecules from fermentation processes, using for this purpose harmless extraction systems, such as the carbohydrates – based ATPS, L-tryptophan partition coefficients were determined, using eq. 8 presented before. The results are presented in Table 6 and Figure 26. Moreover, the composition of the ternary system employed for the L-tryptophan partition studies, as well as the corresponding TLs and TLLs, are also presented in Table 6.

Table 6 - Weight fraction composition and partition coefficients of L-tryptophan in $[C_4mim][CF_3SO_3]$ + carbohydrates + water systems, at 298 K.

Carbohydrates	*Mr*	Weight fraction composition (*wt %*)		TL equation[1]		TLL	$K_{Trp} + \sigma$
		IL	CH	*a*	*b*		
Sucrose	342.31	39.93	25.04	79.53	-1.581	77.30	1.13 ± 0.02
D-glucose	180.16	40.11	24.94	89.86	-1.994	91.40	0.942 ± 0.003
D-(+)-mannose	180.16	39.84	24.91	91.23	-2.063	75.32	0.93 ± 0.04
D-(+)-xylose	150.13	40.08	24.93	88.83	-1.956	53.36	0.84 ± 0.03
Maltitol	344.32	40.00	24.99	101.2	-2.449	99.67	0.94 ± 0.01
Xylitol	152.15	39.82	24.89	92.51	-2.117	84.33	0.94 ± 0.04
D-sorbitol	182.18	39.98	24.97	98.54	-2.345	99.58	0.88 ± 0.04

[1] IL (*wt %*) = $a + b \cdot$CH (*wt %*)

The partition coefficients of L-tryptophan (K_{Trp}) in IL–carbohydrates ATPS have approximately the same magnitude of the usual PEG-polysaccharide systems ($K_{Trp} \approx 1$) reported by Lu et al. [54]. Although the K_i of the carbohydrates are very similar, there are small significant differences between sucrose (the highest partition coefficient), D-(+)-xylose and D-sorbitol (both with the lower partition coefficients) and the remaining carbohydrates. The partition coefficients are further depicted in Figure 26. These differences can be explained by the presence of more hydrophobic/hydrophilic groups on

the carbohydrate constitution. This means that, the more hydrophobic carbohydrate, the lower partition coefficient of the amino acid. Thus, since D-(+)-xylose presents four -OH groups and D-glucose has five -OH groups, D-(+)-xylose is more hydrophobic than D-glucose. These findings are in agreement with Wang et al. [53].

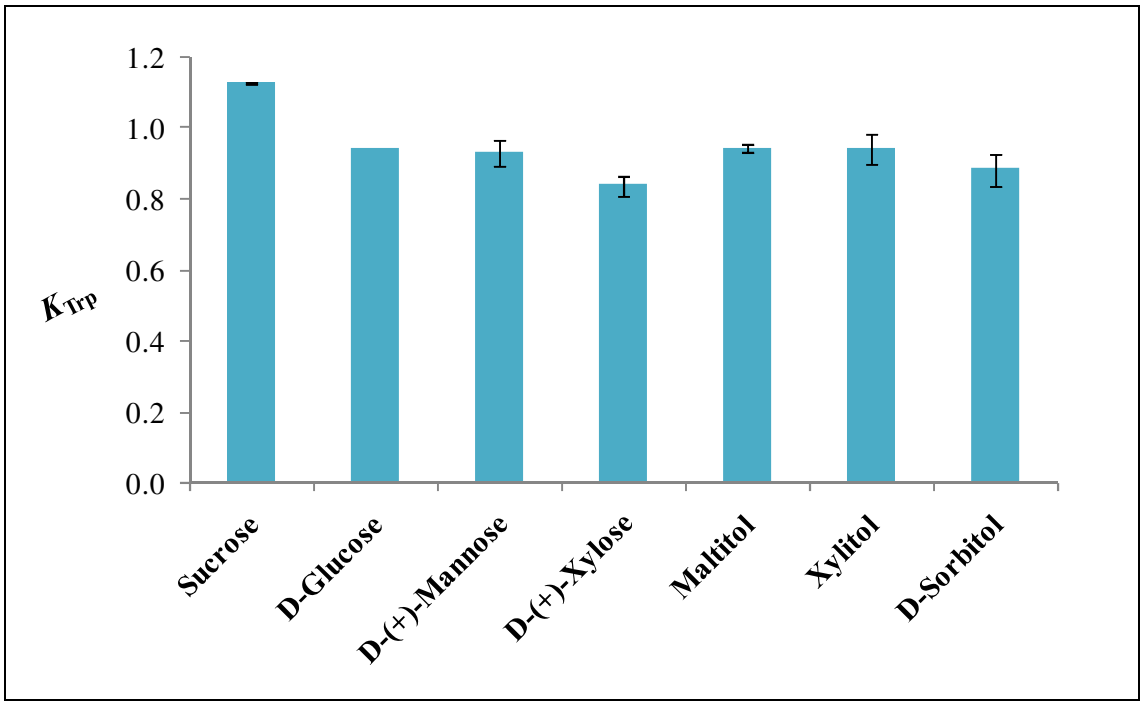

Figure 25 - Partition coefficients of L-tryptophan between the IL and carbohydrates-aqueous rich phases, at 298 K.

3.4. Conclusions

Aqueous systems composed by the studied carbohydrates lactose, maltitol, sucrose, D-sorbitol, D-glucose, D-(+)-galactose, D-(+)-mannose, xylitol, D-(-)-arabinose, L-(+)-arabinose, D-(+)-xylose and the IL [C_4mim][CF_3SO_3] have shown to undergo phase separation. Aqueous phase diagrams between [C_4mim][CF_3SO_3] and carbohydrates were determined and presented. The ability of carbohydrates to induce ATPS formation followed the order: lactose > sucrose > D-glucose > D-(+)-mannose > D-(+)-xylose, while for the alditols follow the order: manitol > D-sorbitol > xylitol. The ability of sugars on the phase separation with hydrophilic ILs allows them to be used in aqueous separation systems, making possible some applications, such as the separation of biomolecules and the recycling of ILs from aqueous systems. Moreover, the benign capacity of carbohydrate-IL-based ABS as prospective extraction media in biotechnological processes was demonstrated by the partition coefficients obtained for L-tryptophan (around 50 % of extraction). Although a higher partition coefficient was obtained with the disaccharide sucrose, for the monosaccharides and polyols the partitions coefficients are similar.

4. General Conclusions

4.1. General Conclusions

Since many biomolecules present narrow tolerance limits of pH, ionic strength, temperature, osmotic pressure and surface charges, the extraction and isolation techniques must be bio-specific and biocompatible. Aqueous two-phase systems (ATPS) result from the incompatibility or immiscibility of polymers and/or salts. Extractive fermentation is an emerging technique that involves the use of ATPS-based *in situ* fermentation processes. The advantages of these processes include the rapid mass transfer due to low-interfacial tension, the facility in operation under continuous mode, the rapid and selective separation, the biocompatibility, separation at room temperature and high yield of biomolecules [19]. Typically, organic volatile solvents (VOCs) have been used in these processes due to their immiscibility in water [19]. As environmental concerns about VOCs increase there is a growing interest in finding environmental friendly replacement solvents for the liquid-liquid separation processes. As alternatives to VOCs appear ILs which have the flexibility to be designed either as hydrophobic or hydrophilic salts. Because ILs are ionic, they may participate directly in the separation mechanism, but can also be tuned *via* different cation/anion combinations to allow for several different separation techniques. Currently, hydrophobic ILs usually contain expensive fluorinated ions which raises the cost of the IL and environmental concern. There are many more, inexpensive, hydrophilic ILs. However these hydrophilic ILs can not be used directly in a liquid- iquid separation with water due to their miscibility at room temperature. Recently, some authors [28] have investigated hydrophilic ILs mixtures with aqueous solutions of inorganic salts to form salt–salt ABS.

In this work, phosphonium and choline-based ILs were studied, allowing the study of the cation nature and the anion identity impact in the ATPS promotion capability. Although there are several reports in literature describing imidazolium-based ILs and inorganic salts ATPS [15, 17, 20], this work is the first evidence that phosphonium and choline-based ILs also allows the phase separation. The representative order of the ability of phase formation was experimentally described: CYPHOS IL 163 < CYPHOS IL 106 < CYPHOS IL 108 < < choline chloride. Moreover, it was concluded that the more distant to the origin is the binodal curve, less salt is needed at the aqueous system to promote the phase split. On the other hand, the farthest from the IL axis is located the binodal curve, the larger the IL salting-out behaviour. The experimental binodal data and the tie-lines (TLs) were fitted by least-squares regression by a gravimetric method described by Merchuck et al. [27]. The

success of the extractive potential of ATPS depends largely of the ability to manipulate phase properties in order to obtain the appropriate partition coefficients and selectivity for the biomolecule of interest, and thus the ATPS investigated were characterized according to their extractive potential for biomolecules, such as β-carotene, caffeine, rhodamine and L-tryptophan. In general, the results indicate that the K_i of the four biomolecules mentioned above increase with the IL hydrophilic nature due to different competing interactions between the IL, the inorganic salt, the biomolecules and water. These results allowed to confirm that L-tryptophan extraction with ILs-based ATPS is much more efficient than the one obtained with conventional PEG-based ATPS [47]. Moreover, the large range obtained in the partition coefficients by changing the IL, indicates that the individual biomolecules extraction efficiency can be manipulated by the correct choice of the IL cation and/or anion.

Phase separation with aqueous solutions of inorganic salts can be considered rather harmful to the environment. Taking this into account and aiming the development of harmless methods for the separation and purification of biomolecules from fermentation processes, carbohydrates-based ATPS were also studied. The results indicate that $[C_4mim][CF_3SO_3]$ + carbohydrates ATPS can be obtained over a large range of concentrations of both IL and carbohydrate. Moreover, it was concluded that disaccharides, such as lactose and sucrose are more efficient in promoting ATPS than monosacharides, and that the inducing ability of alditols for ATPS formation increase with the reduced sugar molecular weight of carbon number. The ability of saccharides to induce ATPS follows the order lactose > sucrose > D-glucose > D-(+)-galactose > D-(+)-mannose > D-(-)-arabinose > L-(+)-arabinose > D-(+)-xylose, while the ability of alditols follows the rank maltitol > D-sorbitol > xylitol. Finally, the conformational isomerism of monosaccharides present some impact through ATPS formation, where L-(+)-arabinose shown to be more efficient than D-(-)-arabinose in supporting the $[C_4mim][CF_3SO_3]$ salting-out. The benign capacity of carbohydrate-IL-based ATPS as prospective extraction media in biotechnological processes was demonstrated by the partition coefficients obtained for L- tryptophan (around 50 % of extraction).

5. References

References

1. Fan, J., Fan, Y.C., Pei, Y.C., Wu, K., Wang, J.J., and Fan, M.H., *Solvent extraction of selected endocrine-disrupting phenols using ionic liquids.* Separation and Purification Technology, 2008. **61**(3): p. 324-331.
2. Zhao, H., Xia, S.Q., and Ma, P.S., *Use of ionic liquids as 'green' solvents for extractions.* Journal of Chemical Technology and Biotechnology, 2005. **80**(10): p. 1089-1096.
3. Jork, C., Seiler, M., Beste, Y.A., and Arlt, W., *Influence of ionic liquids on the phase behavior of aqueous azeotropic systems.* Journal of Chemical and Engineering Data, 2004. **49**(4): p. 852-857.
4. Huddleston, J.G., Willauer, H.D., Swatloski, R.P., Visser, A.E., and Rogers, R.D., *Room temperature ionic liquids as novel media for 'clean' liquid-liquid extraction.* Chemical Communications, 1998(16): p. 1765-1766.
5. McFarlane, J., Ridenour, W.B., Luo, H., Hunt, R.D., DePaoli, D.W., and Ren, R.X., *Room temperature ionic liquids for separating organics from produced water.* Separation Science and Technology, 2005. **40**(6): p. 1245-1265.
6. Soto, A., Arce, A., and Khoshkbarchi, M.K., *Partitioning of antibiotics in a two-liquids phase system formed by water and room temperature ionic liquids.* Separation and Purification Technology, 2005. **44**: p. 242-246.
7. Fadeev, A.G. and Meagher, M.M., *Opportunities for ionic liquids in recovery of bifuels.* Chem. Commun., 2001: p. 295-296.
8. Cull, S.G., Holbrey, J.D., Vargas-Mora, V., Seddon, K.R., and Lye, G.J., *Room temperature ionic liquids as replacements for organic solvents in multiphase bioprocess operations* Biotechnology and Bioengineering, 2000. **69**: p. 227-233.
9. Bridges, N.J., Gutowski, K.E., and Rogers, R.D., *Investigation of aqueous biphasic systems formed from solutions of chaotropic salts with kosmotropic salts (salt-salt ABS).* Green Chemistry, 2007. **9**(2): p. 177-183.
10. Jain, N., Kumar, A., Chauhan, S., and Chauhan, S.M.S., *Chemical and biochemical transformations in ionic liquids.* Tetrahedron, 2005. **61**(5): p. 1015-1060.
11. Qin, W., Wei, H., and Li, S.F.Y., *1,3-Dialkylimidazolium-based room-temperature ionic liquids as background electrolyte and coating material in aqueous capillary electrophoresis.* Journal of Chromatography A, 2003. **985**(1-2): p. 447-454.
12. Plechkova, N.V. and Seddon, K.R., *Applications of ionic liquids in the chemical industry.* Chemical Society Reviews, 2008. **37**: p. 123-150.
13. Dreyer, S. and Kragl, U., *Ionic liquids for aqueous two-phase extraction and stabilization of enzymes.* Biotechnology and Bioengineering, 2008. **99**(6): p. 1416-1424.
14. Du, Z., Yu, Y.L., and Wang, J.H., *Extraction of proteins from biological fluids by use of an ionic liquid/aqueous two-phase system.* Chemistry-a European Journal, 2007. **13**(7): p. 2130-2137.
15. Neves, C.M.S.S., Ventura, S.P.M., Freire, M.G., Marrucho, I.M., and Coutinho, J.A.P., *Evaluation of Cation Influence on the Formation and Extraction Capability of Ionic-Liquid-Based Aqueous Biphasic Systems.* The Journal of Physical Chemistry B, 2009. **113**(15): p. 5194-5199.
16. Pei, Y.C., Wang, J.J., Liu, L., Wu, K., and Zhao, Y., *Liquid-liquid equilibria of aqueous biphasic systems containing selected imidazolium ionic liquids and salts.* Journal of Chemical and Engineering Data, 2007. **52**: p. 2026-2031.

17. Rito-Palomares, M., *Practical application of aqueous two-phase partition to process development for the recovery of biological products.* Journal of Chromatography B, 2004. **807**(1): p. 3-11.
18. Zhang, Y., Zhang, S., Chen, Y., and Zhang, J., *Aqueous biphasic systems composed of ionic liquid and fructose.* Fluid Phase Equilibria, 2007. **257**(2): p. 173-176.
19. Banik, R.M., Santhiagu, A., Kanari, B., Sabarinath, C., and Upadhyay, S.N., *Technological aspects of extractive fermentation using aqueous two-phase systems.* World Journal of Microbiology and Biotechnology, 2003. **19**(4): p. 337-348.
20. Gutowski, K.E., Broker, G.A., Willauer, H.D., Huddleston, J.G., Swatloski, R.P., Holbrey, J.D., and Rogers, R.D., *Controlling the Aqueous Miscibility of Ionic Liquids: Aqueous Biphasic Systems of Water-Miscible Ionic Liquids and Water-Structuring Salts for Recycle, Metathesis, and Separations.* Journal of the American Chemical Society, 2003. **125**(22): p. 6632-6633.
21. Kubisa, P., *Application of ionic liquids as solvents for polymerization processes.* Progress in Polymer Science, 2004. **29**(1): p. 3-12.
22. Toh, S.L.I., McFarlane, J., Tsouris, C., DePaoli, D.W., Luo, H., and Dai, S., *Room-temperature ionic liquids in liquid-liquid extraction: Effects of solubility in aqueous solutions on surface properties.* Solvent Extraction and Ion Exchange, 2006. **24**(1): p. 33-56.
23. Wu, B., Zhang, Y., and Wang, H., *Phase Behavior for Ternary Systems Composed of Ionic Liquid + Saccharides + Water.* The Journal of Physical Chemistry B, 2008. **112**(20): p. 6426-6429.
24. Wu, B., Zhang, Y., Wang, H., and Yang, L., *Temperature Dependence of Phase Behavior for Ternary Systems Composed of Ionic Liquid + Sucrose + Water.* The Journal of Physical Chemistry B, 2008. **112**(41): p. 13163-13165.
25. Wu, B., Zhang, Y.M., and Wang, H.P., *Aqueous biphasic systems of hydrophilic ionic liquids plus sucrose for separation.* Journal of chemical and engineering data, 2008. **53**(4): p. 983-985.
26. Najdanovic-Visak, V., Rebelo, L.P.N., and da Ponte, M.N., *Liquid-liquid behaviour of ionic liquid-1-butanol-water and high pressure CO2-induced phase changes.* Green Chemistry, 2005. **7**(6): p. 443-450.
27. Merchuk, J.C., Andrews, B.A., and Asenjo, J.A., *Aqueous two-phase systems for protein separation: Studies on phase inversion.* Journal of Chromatography B: Biomedical Sciences and Applications, 1998. **711**(1-2): p. 285-293.
28. CAREY, F.A., *ORGANIC CHEMISTRY*. p. 1011-1055.
29. Treszczanowicz;, T.T.T.K.-G.D.C.a.A.J., *Distribution coefficient of β-carotene between an organic solvent and water.* 1998. **43**(4): p. 632-634.
30. Kubin, R.F. and Fletcher, A.N., *Fluorescence quantum yields of some rhodamine dyes.* J. Luminescence 1982. **27**: p. 455.
31. Li, S., He, C., Liu, H., Li, K., and Liu, F., *Ionic liquid-based aqueous two-phase system, a sample pretreatment procedure prior to high-performance liquid chromatography of opium alkaloids.* Journal of Chromatography B, 2005. **826**(1-2): p. 58-62.
32. Dewick, P.M., *Medicinal Natural Products*. 2002. p. 394-396.
33. Majewski, P., Pernak, A., Grzymislawski, M., Iwanik, K., and Pernak, J., *Ionic liquids in embalming and tissue preservation. Can traditional formalin-fixation be replaced safely?* Acta Histochemica, 2003. **105**(2): p. 135-142.

34. Bradaric, C.J., Downard, A., Kennedy, C., Robertson, A.J., and Zhou, Y.H., *Industrial preparation of phosphonium ionic liquids.* Green Chemistry, 2003. **5**(2): p. 143-152.
35. Marták, J. and Schlosser, S., *Extraction of lactic acid by phosphonium ionic liquids.* Separation and Purification Technology, 2007. **57**(3): p. 483-494.
36. Nockemann, P., Thijs, B., Driesen, K., Janssen, C.R., Van Hecke, K., Van Meervelt, L., Kossmann, S., Kirchner, B., and Binnemans, K., *Choline Saccharinate and Choline Acesulfamate: Ionic Liquids with Low Toxicities.* The Journal of Physical Chemistry B, 2007. **111**(19): p. 5254-5263.
37. Andrew P. Abbott, G.C.D.L.D.R.K.R., *Ionic Liquid Analogues Formed from Hydrated Metal Salts.* Chemistry - A European Journal, 2004. **10**(15): p. 3769-3774.
38. Abbott, A.P., Capper, G., Davies, D.L., Munro, H.L., Rasheed, R.K., and Tambyrajah, V., *Preparation of novel, moisture-stable, Lewis-acidic ionic liquids containing quaternary ammonium salts with functional side chains.* Chemical Communications, 2001(19): p. 2010-2011.
39. Abbott, A.P., Capper, G., Davies, D.L., and Rasheed, R., *Ionic Liquids Based upon Metal Halide/Substituted Quaternary Ammonium Salt Mixtures.* Inorganic Chemistry, 2004. **43**(11): p. 3447-3452.
40. Abbott, A.P., Capper, G., Davies, D.L., Rasheed, R.K., and Tambyrajah, V., *Novel solvent properties of choline chloride/urea mixtures.* Chemical Communications, 2003(1): p. 70-71.
41. Cooper, E.R., Andrews, C.D., Wheatley, P.S., Webb, P.B., Wormald, P., and Morris, R.E., *Ionic liquids and eutectic mixtures as solvent and template in synthesis of zeolite analogues.* Nature, 2004. **430**(7003): p. 1012-1016.
42. Li, X., Hou, M., Han, B., Wang, X., and Zou, L., *Solubility of CO2 in a Choline Chloride + Urea Eutectic Mixture.* Journal of Chemical & Engineering Data, 2008. **53**(2): p. 548-550.
43. Galaev, I.Y. and Mattiasson, B., Enzyme Microbiol. Technol., 1993. **15**: p. 354.
44. Willauer, H.D., Huddleston, J.G., and Rogers, R.D., *Solute partitioning in aqueous biphasic systems composed of polyethylene glycol and salt: The partitioning of small neutral organic species.* Industrial & Engineering Chemistry Research, 2002. **41**(7): p. 1892-1904.
45. Deng, Y.F., Chen, J., and Zhang, D.L., *Phase diagram data for several salt plus salt aqueous biphasic systems at 298.15 K.* Journal of Chemical and Engineering Data, 2007. **52**(4): p. 1332-1335.
46. Ventura, S.P.M., Neves, C.M.S.S., Freire, M.G., Marrucho, I.M., Oliveira, J., and Coutinho, J.A.P., *Evaluation of Anion Influence on the Formation and Extraction Capacity of Ionic-Liquid-Based Aqueous Biphasic Systems.* The Journal of Physical Chemistry B, 2009. **113**(27): p. 9304-9310.
47. Salabat, A., Abnosi, M.H., and Motahari, A., *Investigation of Amino Acid Partitioning in Aqueous Two-Phase Systems Containing Polyethylene Glycol and Inorganic Salts.* Journal of Chemical & Engineering Data, 2008. **53**(9): p. 2018-2021.
48. Jianji Wang, Y.P., Yang Zhao and Zhiguo Hu, *Recovery of amino acids by imidazolium based ionic liquids from aqueous media.* Green Chemistry, 2005. **7**: p. 196 - 202.

49. Fadeev, A.G. and Meagher, M.M., *Opportunities for ionic liquids in recovery of biofuels.* Chemical Communications, 2001(03): p. 295-296.
50. Wang, J., Pei, Y., Zhao, Y., and Hu, Z., Green Chem., 2005. **7**: p. 196.
51. Lungwitz, R., M. Friedrich, W. Linert, and S. Spange, *Polarity of Ionic Liquids.* New J. Chem, September 2008 **32** p. 1457–1644.
52. Galema, S.A., Blandamer, M.J., and Engberts, J.B.F.N., *Stereochemical aspects of hydration of carbohydrates in aqueous solutions. 2. Kinetic medium effects.* The Journal of Organic Chemistry, 1992. **57**(7): p. 1995-2001.
53. Huddleston, J.G., Willauer, H.D., and Rogers, R.D., J. Chem. Eng. Data, 2003. **48**: p. 1230.
54. Lu, M. and Tjerneld, F., *Interaction between tryptophan residues and hydrophobically modified dextran: Effect on partitioning of peptides and proteins in aqueous two-phase systems.* Journal of Chromatography A, 1997. **766**(1-2): p. 99-108.

Appendix A

Calibration Curves

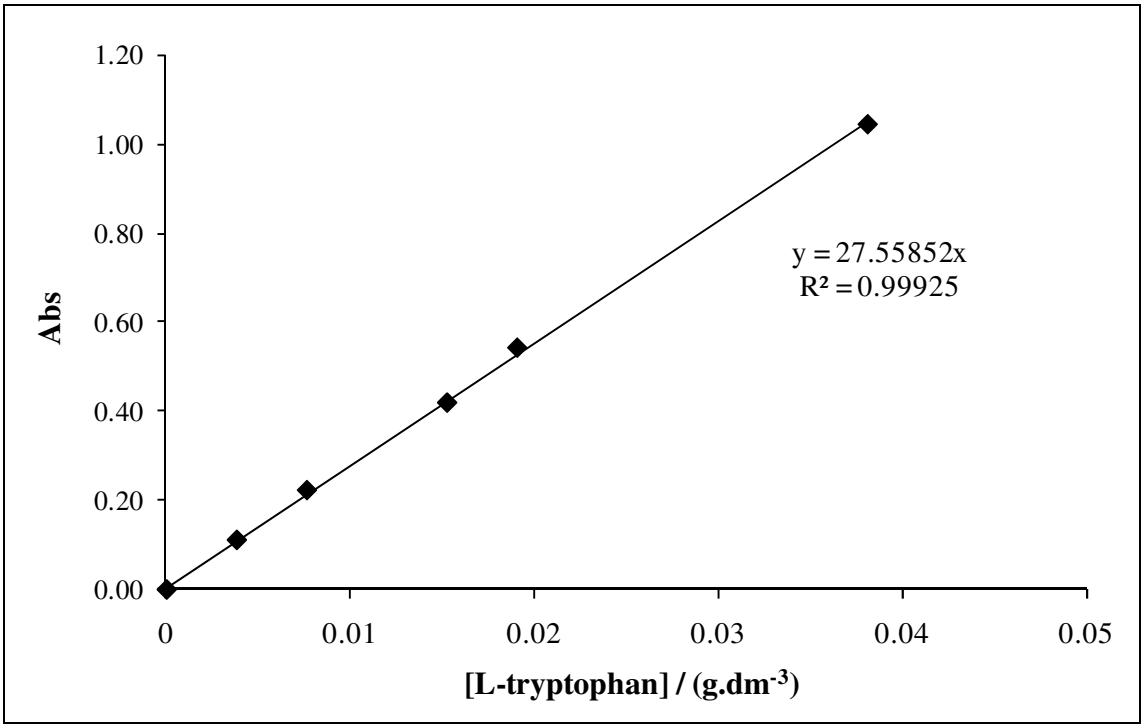

Figure A 1 - Calibration curve for L-tryptophan at λ = 279 nm.

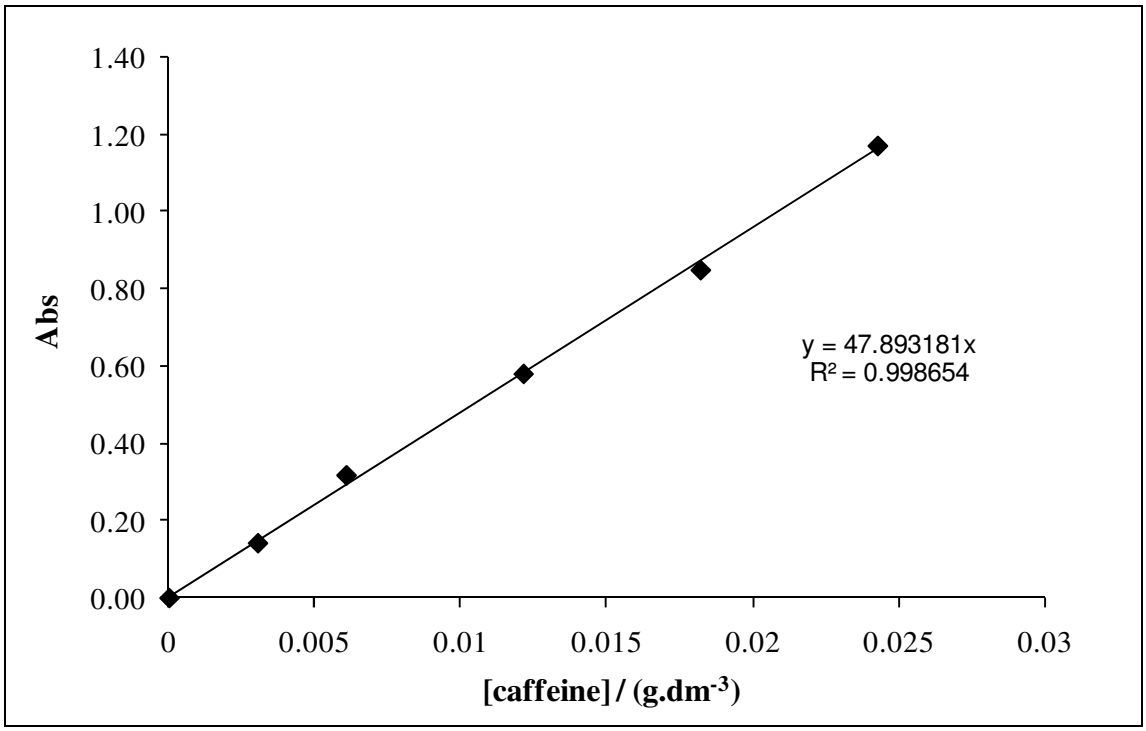

Figure A 2 - Calibration curve for caffeine at λ = 274 nm.

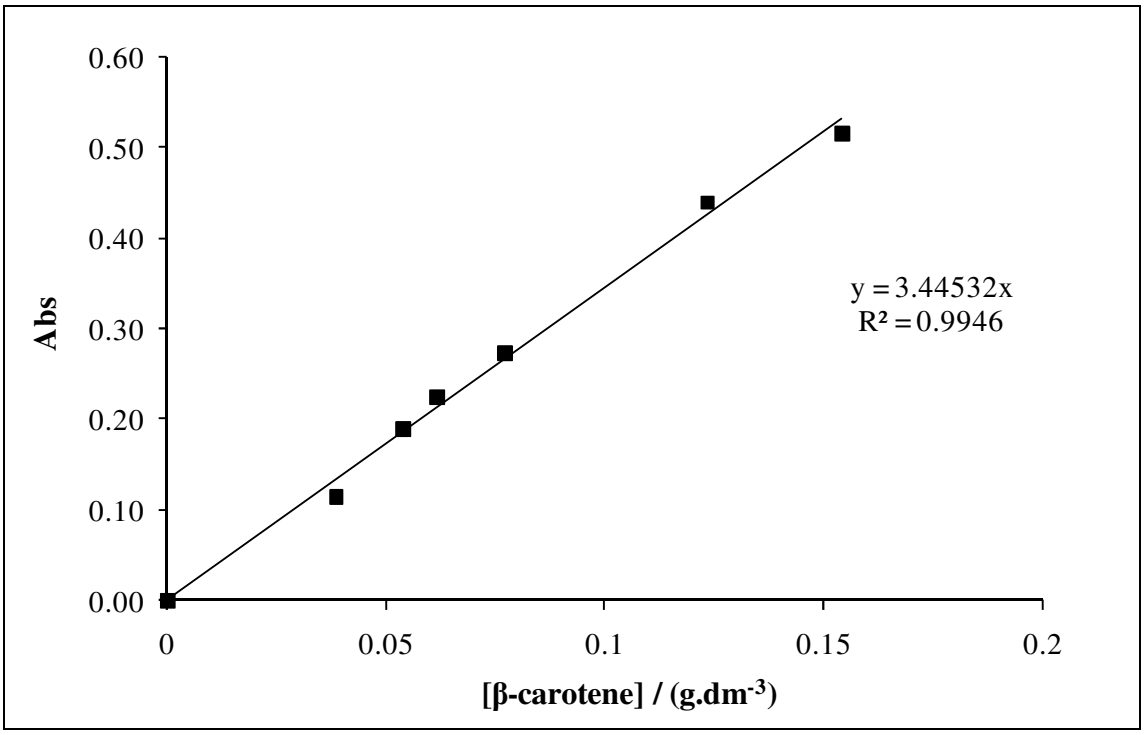

Figure A 3 - Calibration curve for β-carotene at λ = 512 nm.

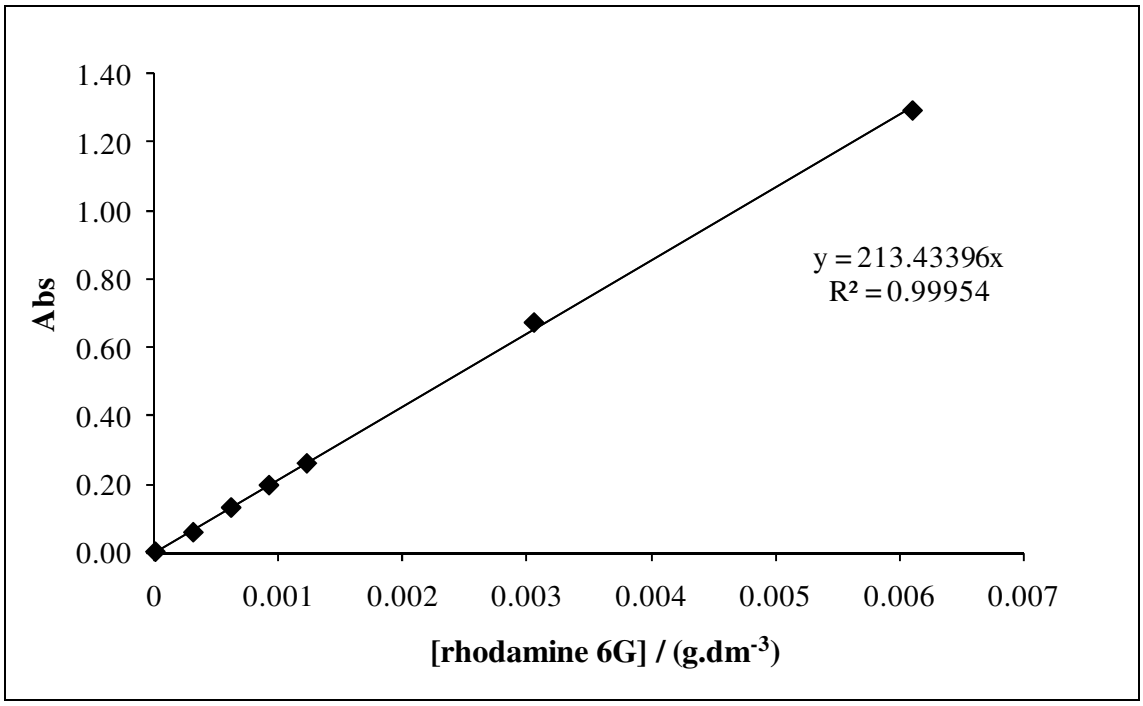

Figure A 4 - Calibration curve for rhodamine 6G at λ = 527 nm.

Appendix B

Experimental Data of Binodal Curves

Table B 1 - Experimental binodal curve mass fraction data for the system IL (1) + K_3PO_4 (2) + H_2O (3) at 298 K.

[C_4mim][Cl] + K_3PO_4			
100 w_1	100 w_2	100 w_1	100 w_2
22.7962	12.0713	8.0235	24.8867
21.2266	13.2594	7.6480	25.2671
19.6295	14.4317	7.1521	25.8415
17.7632	15.9162	6.7346	26.3186
16.6104	16.6060	6.3288	26.8137
15.3358	17.5821	5.9863	27.2177
13.9601	18.8572	5.6349	27.6678
12.9821	19.6394	5.3135	28.1063
11.0827	22.0193	4.9766	28.6101
10.4256	22.5596	4.5074	29.3474
9.7921	23.1133	3.8039	30.5210
9.1132	23.8032	2.9124	32.1567
8.5295	24.4075		

Table B 2 - Experimental binodal curve mass fraction data for the system IL (1) + K_3PO_4 (2) + H_2O (3) at 298 K.

CYPHOS IL 108					
100 w_1	100 w_2	100 w_1	100 w_2	100 w_1	100 w_2
77.5934	0.90771	11.2609	14.4430	7.4775	17.1636
53.4656	1.5792	11.2103	14.5451	7.4469	17.1578
25.9023	7.2379	11.0322	14.6659	7.3744	17.2109
18.2881	11.4349	10.9383	14.7164	7.3094	17.2570
17.9208	11.4616	10.8315	14.7398	7.2174	17.3563
17.4714	11.7238	10.7604	14.7986	7.1409	17.3780
17.1359	11.7926	10.6804	14.8402	7.0842	17.4493
16.9415	11.9094	10.5979	14.8798	7.0141	17.4787
16.7287	11.9991	10.4992	15.0632	6.9281	17.6240
16.5239	12.1081	10.4027	15.0715	6.8851	17.5459
16.3093	12.2274	10.2866	15.2087	6.6925	18.0071
16.0326	12.2485	10.1696	15.1612	6.5704	17.9871
15.8815	12.3688	10.0974	15.1936	6.4922	17.9813
15.7122	12.4548	10.0264	15.2281	6.4232	18.0218
15.5477	12.5460	9.9546	15.2601	6.3594	18.0536
15.3678	12.6077	9.8942	15.3046	6.2947	18.0826
15.2070	12.6873	9.8279	15.3474	6.2293	18.1219
14.9984	12.7611	9.7574	15.3750	6.1590	18.1035
14.8520	12.8584	9.6942	15.3936	6.1033	18.1352
14.5301	13.0061	9.6382	15.4562	6.0215	18.3160
14.3171	13.0385	9.5057	15.5441	5.9277	18.4942
14.1604	13.1165	9.4206	15.5440	5.8285	18.6036
14.0185	13.1889	9.3527	15.5680	5.7511	18.6721
13.8758	13.2791	9.2936	15.6016	5.6735	18.7119
13.7015	13.3035	9.2257	15.6554	5.6080	18.7912
13.5581	13.3816	9.1053	15.7240	5.5372	18.8673
13.4310	13.4522	8.9754	15.8082	5.4743	18.9215
13.2930	13.5466	8.6569	16.4467	5.4140	18.9163

13.1275	13.5644	8.5488	16.4900	5.3627	18.9361
12.9994	13.6333	8.4453	16.5391	5.2760	19.0394
12.8554	13.6283	8.3687	16.6413	5.2150	19.1205
12.7431	13.7052	8.2877	16.6178	5.0581	19.4294
12.6331	13.7689	8.2414	16.6429	4.9745	19.4137
12.4280	13.8984	8.1978	16.6689	4.8979	19.4868
12.2211	14.0268	8.1218	16.7586	4.8186	19.5608
12.0649	14.0426	8.0307	16.8020	4.7515	19.5266
11.8794	14.1976	7.9690	16.8060	4.6646	19.5781
11.7391	14.2035	7.8985	16.9016	4.5839	19.6828
11.6483	14.2683	7.8380	16.9003	4.5041	19.7926
11.5457	14.3293	7.7460	16.9424	4.3991	19.9380
11.4515	14.3768	7.6696	17.0048		
11.3520	14.4131	7.5775	17.0471		

Table B 3 - Experimental binodal curve mass fraction data for the system IL (1) + K_3PO_4 (2) + H_2O (3) at 298 K.

CYPHOS IL 106					
100 w_1	100 w_2	100 w_1	100 w_2	100 w_1	100 w_2
74.4669	2.2202	22.8277	7.7423	14.3469	10.1989
67.4773	2.3077	22.3282	7.8540	14.1357	10.2886
58.0248	2.4925	21.8518	8.0193	13.9193	10.3549
53.5776	2.7414	21.4753	8.1345	13.7196	10.4010
48.7133	3.1715	21.0918	8.2422	13.5446	10.4780
44.9736	3.5279	20.6399	8.3646	13.3608	10.5060
42.3789	3.6745	20.2732	8.4854	13.1813	10.6004
40.8264	3.9382	19.9194	8.6000	12.6225	11.7626
39.1193	4.0598	19.5592	8.6908	12.4667	11.8557
37.5562	4.4154	19.2960	8.7900	12.3861	11.9011
36.4299	4.5422	18.9100	8.8664	12.2416	11.9042
35.4062	5.0843	18.5885	8.9294	11.9046	12.2069
33.7752	5.2535	18.2399	9.0434	11.5277	12.4746
32.5931	5.5612	17.9236	9.1328	111538	12.5346
31.4726	5.8212	17.6326	9.1890	10.5211	12.8956
30.4335	5.9335	17.3896	9.2839	10.4392	12.9751
29.5478	6.1652	17.1279	9.3565	10.3117	12.9941
28.6989	6.3695	16.8371	9.4172	10.1983	13.0476
27.9071	6.4466	16.6273	9.6111	10.1069	13.0892
27.5036	6.5847	16.2956	9.6472	9.9947	13.1498
26.9968	6.6327	16.0398	9.6882	9.9092	13.3205
26.5317	6.8526	15.7765	9.7467	9.7609	13.3717
25.9397	6.9643	15.5817	9.8520	9.6275	13.3519
25.3647	7.0663	15.3584	9.8935	9.5221	13.3822
24.7525	7.2321	15.1536	9.9358	9.4700	13.3938
24.2198	7.4007	15.0031	10.0231	9.3748	13.4448
23.7150	7.5404	14.7489	10.0640		
23.2349	7.6537	14.5995	10.1546		

Table B 4 - Experimental binodal curve mass fraction data for the system IL (1) + K_3PO_4 (2) + H_2O (3) at 298 K.

CYPHOS IL 163		**Choline chloride**	
100 w_1	100 w_2	100 w_1	100 w_2
75.4870	1.2685	78.6275	0.7012
56.9866	2.1040	63.1347	2.2302
53.0380	2.5415	47.6190	7.4111
9.2818	8.6649	42.4002	8.8205
		37.6349	11.3617
		35.1909	12.8118
		30.7881	15.9059
		22.4317	21.8632
		18.5374	24.8462

Appendix C

Binodal Curves and TLs

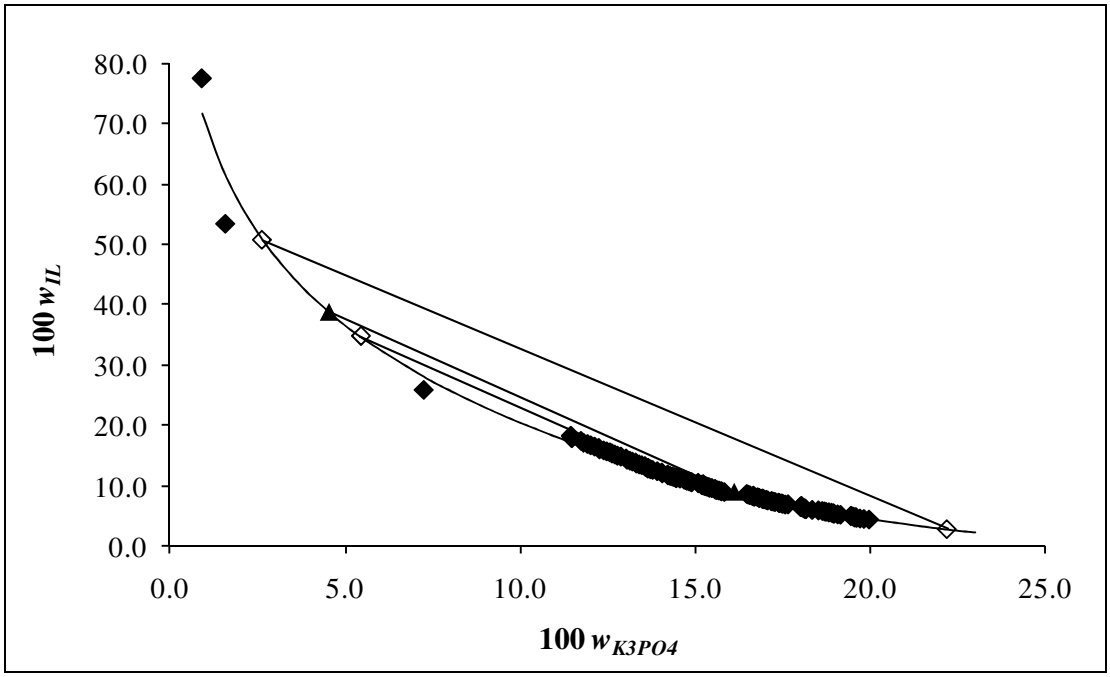

Figure C 1 - Phase diagram for CYPHOS IL 108 based ternary systems composed by IL + K_3PO_4 + H_2O at 298 K: ♦, experimental binodal data; ▲, extraction TL data; ◊, TL data; ▬, Fitting of experimental data by eq. 1.

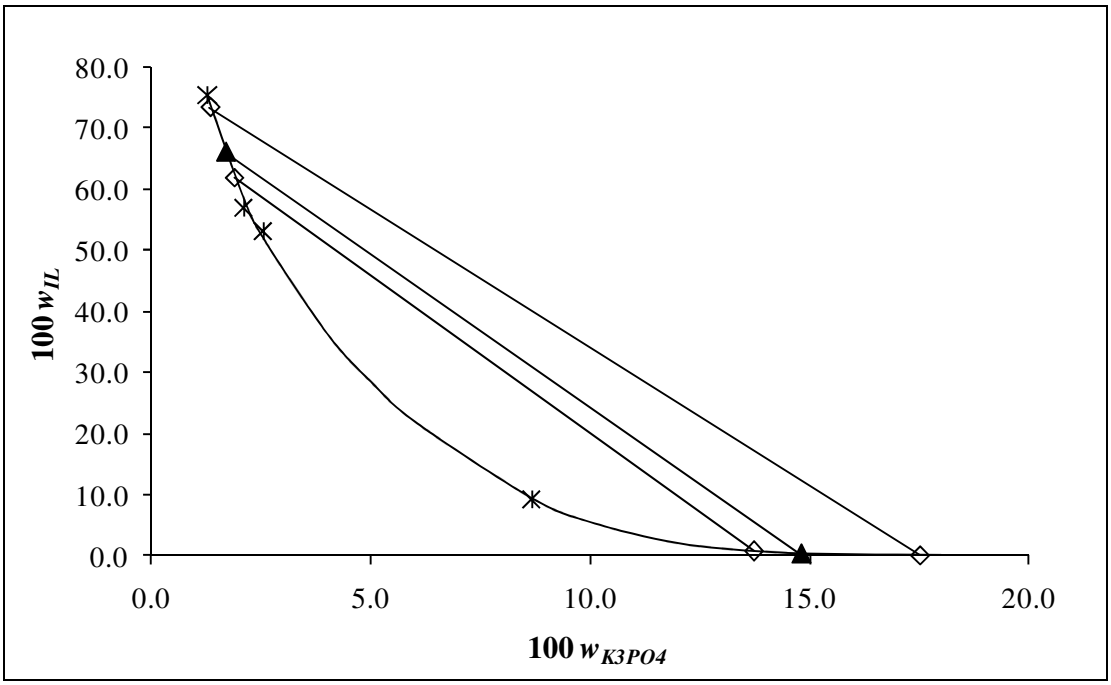

Figure C 2 - Phase diagram for CYPHOS IL 163 based ternary systems composed by IL + K_3PO_4 + H_2O at 298 K: ∗, experimental binodal data; ▲, extraction TL data; ◊, TL data; ▬, Fitting of experimental data by eq. 1.

Appendix D

Experimental Data of Binodal Curves

Table D 1 - Experimental binodal curve mass fraction data for the system IL (1) + Carbohydrate (2) + H_2O (3) at 298 K.

[C_4mim][BF_4] + D-glucose					
100 w_1	100 w_2	100 w_1	100 w_2	100 w_1	100 w_2
75.2490	2.3881	42.6559	7.2106	29.3483	11.5547
69.5549	2.7588	41.7287	7.3923	28.1486	12.2326
61.9341	3.1640	40.1697	7.9731	27.6645	12.3563
58.6109	3.6582	38.8417	8.1598	26.9900	12.6071
55.7919	4.1364	38.1173	8.4512	26.1826	12.9443
54.3738	4.6568	37.0907	8.6863	25.2259	13.4309
51.8934	4.9979	36.2404	8.9089	24.6248	13.7502
50.3331	5.4134	34.9962	9.3866	23.4952	14.2296
48.7944	5.8286	34.2781	9.5627	22.9090	14.4825
47.5904	6.1589	33.1269	10.0651	22.2102	14.8670
46.4157	6.4488	32.5508	10.3047	21.3839	15.3856
45.1486	6.7504	31.5326	10.7079	20.2697	16.1556
43.9957	6.9891	30.6353	11.1175	18.7835	17.3431
43.3360	6.9321	30.0518	11.2224		

Table D 2 - Experimental binodal curve mass fraction data for the system $[C_4mim][CF_3SO_3]$ (1) + Carbohydrate (2) + H_2O (3) at 298 K.

D-glucose				**D-(+)-mannose**	
100 w_1	100 w_2	100 w_1	100 w_2	100 w_1	100 w_2
70.7134	5.0360	28.3764	18.0857	64.8760	8.6316
64.3492	6.2705	27.5034	18.6608	60.8706	9.8346
61.7235	6.9267	27.0186	18.8968	56.0231	11.1787
58.1970	7.7439	26.4837	19.0622	52.5818	12.0626
55.7481	8.6443	25.9630	19.2585	50.0435	12.9785
52.6220	9.3564	25.3938	19.5034	47.7135	13.8156
50.6149	10.2228	24.5757	20.0296	44.1636	15.6639
48.4233	10.8946	23.9266	20.4443	40.5916	16.7527
45.9950	11.4381	23.1254	20.8964	37.6191	18.0734
44.5421	11.9688	22.3935	21.1928	36.2642	18.5303
42.6894	12.4911	21.4186	21.7287	35.0096	19.0113
40.2582	13.5371	20.7408	22.4421	33.5765	19.9550
38.6869	13.9254	20.0030	22.9040	31.4894	20.6602
37.2662	14.3704	19.1299	23.6147	29.8256	21.1205
35.3999	15.3018	18.3079	24.3028	28.1054	21.8247
34.2066	15.5314	17.4040	25.0572	26.6704	22.4546
33.3388	15.8956	16.6407	25.8189	25.4045	23.5145
32.5622	16.2527	15.7532	26.4985	24.0254	24.1517
31.7911	16.5735	15.0095	27.2795	22.9965	24.9679
31.0485	16.9157	13.3303	29.6538	22.0136	25.7172
30.0063	17.6089			21.1057	26.4960
28.9851	17.7711			18.9369	28.5630

Table D 3 - Experimental binodal curve mass fraction data for the system $[C_4mim][CF_3SO_3]$ (1) + Carbohydrate (2) + H_2O (3) at 298 K.

Sucrose		**D-(+)-galactose**		**D-(+)-xylose**	
100 w_1	100 w_2	100 w_1	100 w_2	100 w_1	100 w_2
74.3274	4.7415	61.0577	8.5350	71.1398	11.2673
67.1500	8.0108	53.9164	10.3804	60.7959	14.2226
59.4327	11.1230	49.8546	11.6739	52.7070	16.7697
54.2610	13.9984	47.6505	12.0803	49.1522	17.9019
48.2106	17.1882	45.8982	12.5601	47.0747	18.2635
42.9105	19.7401	43.4384	13.3009	42.3666	20.5517
38.6476	21.9081	42.1389	13.5979	39.2347	21.9157
36.3353	23.0929	39.8369	14.3225	36.4560	23.3348
33.9343	24.1365	37.2042	15.4268	34.2809	24.5801
32.1461	25.1415	35.3321	15.9414	32.0368	25.5128
30.2199	26.2322	33.6419	16.4526	28.8826	27.3117
28.4796	27.0827	32.0630	16.9974	26.1274	29.0555
26.2117	28.8490	30.7531	17.3317	23.0186	31.3867
24.6119	29.7415	29.0297	18.0390		
23.1022	30.3751	27.4236	18.7043		
21.8276	30.8582	26.0478	19.2676		
20.7967	31.3714	24.7474	19.8680		
19.5364	32.1294	23.6037	20.3399		
18.1972	32.9929	22.2887	21.0732		
16.8570	34.0624	20.3385	22.3792		
15.6073	34.9902	17.6472	23.9326		
14.3367	36.1600				
13.3585	36.6955				

Table D 4 - Experimental binodal curve mass fraction data for the system $[C_4mim][CF_3SO_3]$ (1) + Carbohydrate (2) + H_2O (3) at 298 K.

D-(+)-lactose		**D-(-)-arabinose**		**L-(+)-arabinose**	
100 w_1	100 w_2	100 w_1	100 w_2	100 w_1	100 w_2
85.3916	0.7329	64.7475	9.8217	53.0112	13.0506
73.9003	1.3918	589833	10.8809	49.7286	13.7781
57.3669	2.3050	51.1611	12.3168	41.3169	17.3279
48.8293	4.6954	48.7887	12.9662	31.1939	22.1602
		42.6944	15.2084		
		38.0847	17.0765		
		35.6884	17.9848		
		33.7642	18.6584		
		29.3007	20.6024		

Table D 5 - Experimental binodal curve mass fraction data for the system $[C_4mim][CF_3SO_3]$ (1) + Carbohydrate (2) + H_2O (3) at 298 K.

D-sorbitol					
100 w_1	100 w_2	100 w_1	100 w_2	100 w_1	100 w_2
74.9096	3.7490	23.6560	15.7227	18.7622	18.4855
68.0337	4.7991	23.1053	15.9685	18.5298	18.6713
59.4219	5.9384	22.6068	16.2423	18.3222	18.7914
49.7353	7.8828	22.2587	16.5272	18.0880	19.0002
46.3405	8.4806	21.7839	16.7670	17.8703	19.1659
41.8341	9.8748	21.4098	17.0359	17.6702	19.3176
39.7041	10.4579	25.8859	14.6851	17.4579	19.4900
38.2130	11.1464	25.1886	14.9844	17.0771	19.8455
36.2173	11.6004	24.4093	15.2615	16.6846	20.1980
34.7903	12.0948	23.6560	15.7227	16.3265	20.4439
33.2935	12.4954	23.1053	15.9685	16.0123	20.9377
32.0710	12.7241	22.6068	16.2423	15.6536	21.1152
31.0922	13.1690	22.2587	16.5272	15.3313	21.3402
30.1590	13.5795	21.7839	16.7670	14.9462	21.8136
29.1104	13.8461	21.4098	17.0359	14.5243	22.1686
28.0745	14.1190	21.0254	17.1890	14.0973	22.6234
27.2552	14.4588	20.7149	17.4249	13.6865	23.2004
26.4981	14.7233	20.4010	17.7108	13.3420	23.6259
25.8859	14.6851	19.8448	18.1507	12.9988	23.9657
25.1886	14.9844	19.4900	18.2379	12.6596	24.5508
24.4093	15.2615	19.1269	18.3398	12.2026	25.2312

Table D 6 - Experimental binodal curve mass fraction data for the system $[C_4mim][CF_3SO_3]$ (1) + Carbohydrate (2) + H_2O (3) at 298 K.

Xylitol		**Maltitol**	
100 w_1	100 w_2	100 w_1	100 w_2
62.6714	8.3585	54.8079	7.8548
55.5502	9.0249	51.9000	8.4511
52.7933	9.6272	49.9130	9.1633
50.7670	10.4605	48.2806	9.7058
48.5804	11.0805	46.8608	10.2044
47.0210	11.6472	45.2655	10.9138
45.3914	12.0493	43.4272	11.5069
44.1771	12.5082	41.6827	11.9421
42.8884	13.0232	40.5688	12.4437
41.4088	13.8610	39.4314	12.9004
39.1433	14.4843	38.4387	13.2785
38.1662	14.9427	37.2271	13.7001
36.2432	15.6894	36.2492	14.2311
35.1609	16.0345	35.0775	14.5263
34.3984	16.2903	33.5786	15.2078
33.7361	16.5732	32.7302	15.6428
33.2149	16.6177	32.0381	15.8854
32.6062	16.8379	31.0797	16.0088
31.6116	17.5384	30.6071	16.4065
30.5188	18.1252	30.0629	16.7562
29.4471	18.4590	29.0169	17.2683
28.6101	18.9560	28.4283	17.5061
27.8868	19.4053	27.8844	17.7498
27.0447	19.7795	27.1153	18.3293
26.3456	20.0180	25.9676	19.0724
25.7138	20.5290	24.8538	19.7420
25.0842	20.9759	23.7822	20.2202
24.3019	21.3390	22.7888	20.8741

23.3643	21.9166	21.9097	21.3121
22.9169	22.2519	21.0976	21.9887
22.3911	22.5256	19.9741	22.9473
21.8361	22.8375	18.5042	24.3256
21.2886	23.3252	17.5070	25.4455
20.7119	23.7061		
19.9608	24.2377		
19.2521	24.8227		
18.5856	25.2703		
17.7810	26.1869		
17.2505	26.6424		
16.1613	27.9642		
14.4099	30.7247		

Appendix E

Binodal Curves and TL

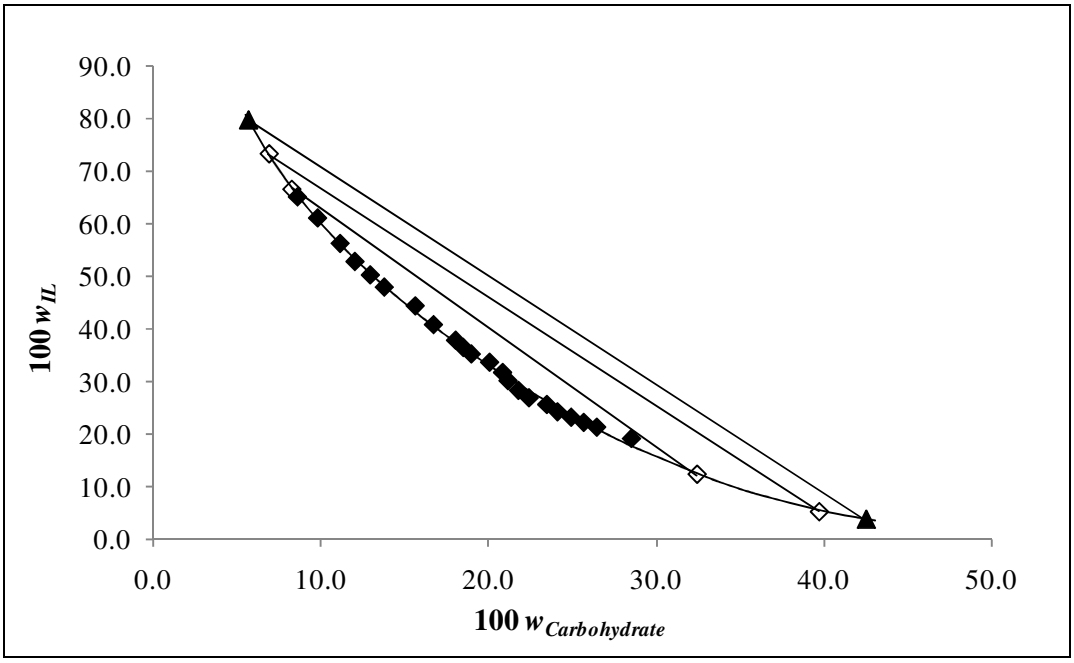

Figure E 1 - Phase diagram for D-(+)-mannose based ternary systems composed by Saccharides + $[C_4mim][CF_3SO_3]$ + H_2O at 298 K: ♦, D-(+)-mannose; ▲, extraction TL data; ◊, TL data; ▬, Fitting of experimental data by eq. 1.

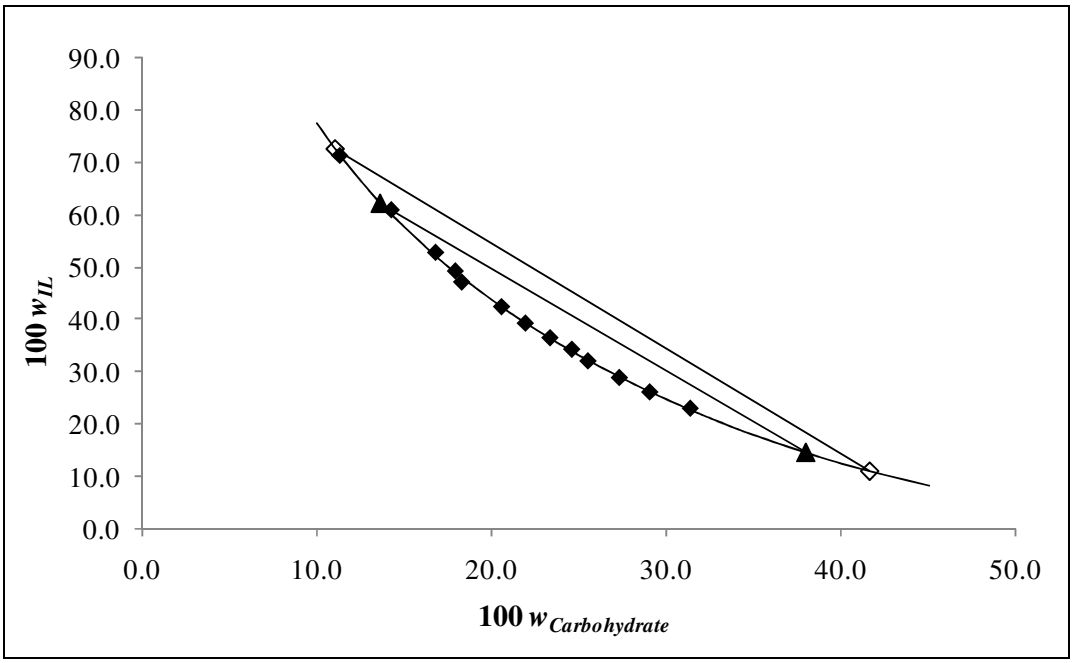

Figure E 2 - Phase diagram for D-(+)-xylose based ternary systems composed by Saccharides + $[C_4mim][CF_3SO_3]$ + H_2O at 298 K: ♦, D-(+)-xylose; ▲, extraction TL data; ◊, TL data; ▬, Fitting of experimental data by eq. 1.

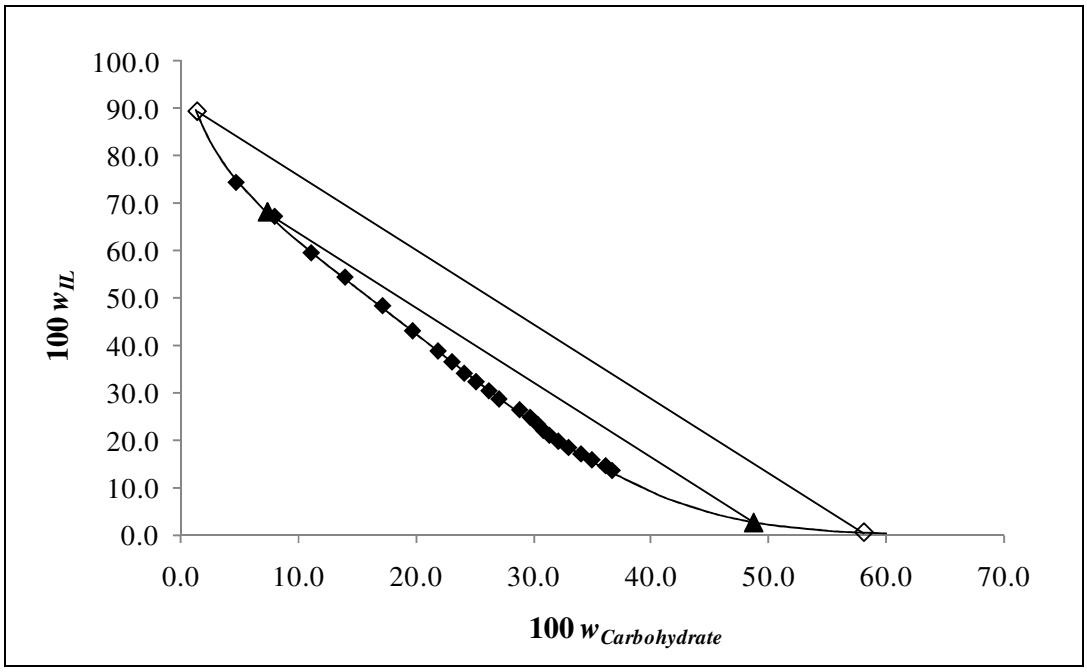

Figure E 3 - Phase diagram for sucrose based ternary systems composed by Saccharides + $[C_4mim][CF_3SO_3]$ + H_2O at 298 K: ♦, sucrose; ▲, extraction TL data; ◊, TL data; ▬, Fitting of experimental data by eq. 1.

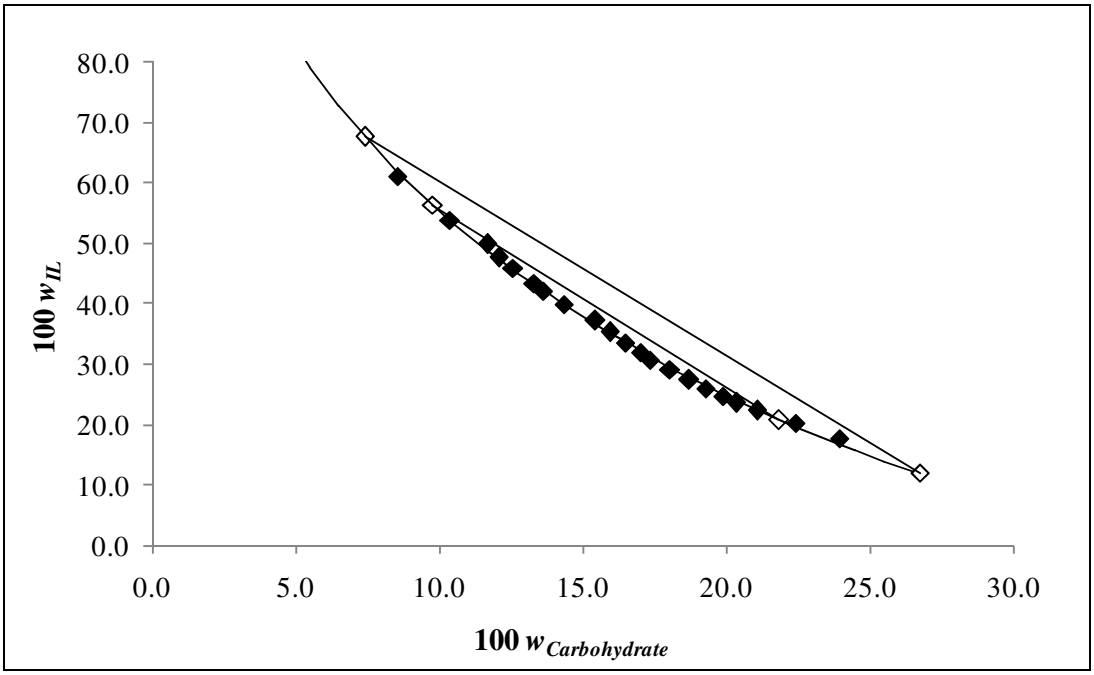

Figure E 4 - Phase diagram for D-(+)-galactose based ternary systems composed by Saccharides + $[C_4mim][CF_3SO_3]$ + H_2O at 298 K: ♦, D-(+)-galactose; ◊, TL data; ▬, Fitting of experimental data by eq. 1**.**

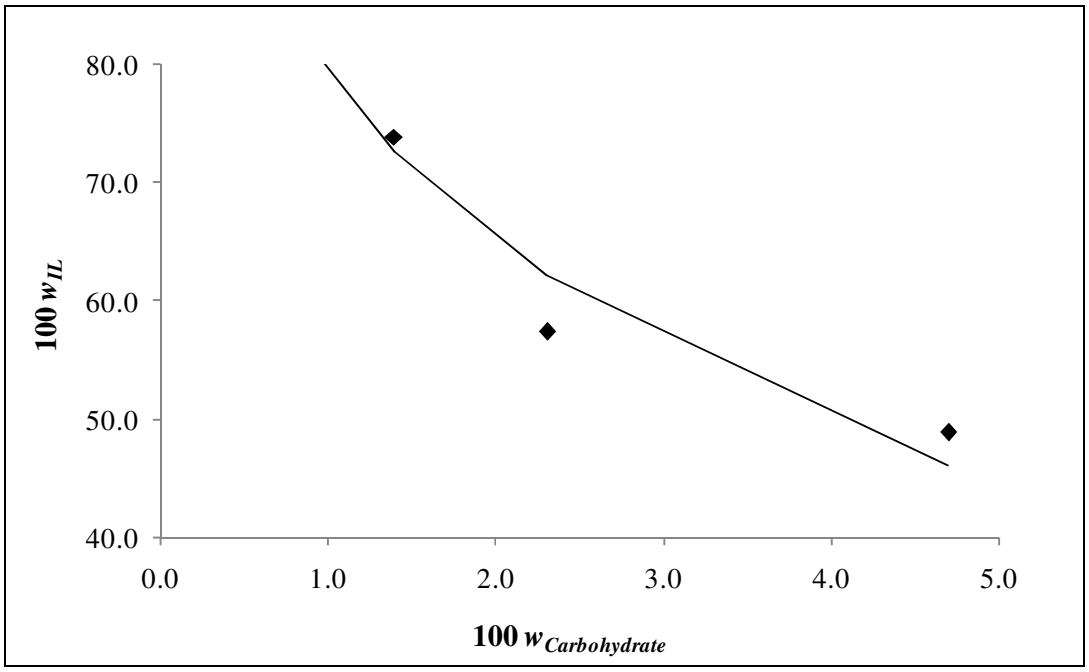

Figure E 5 - Phase diagram for lactose based ternary systems composed by Saccharides + $[C_4mim][CF_3SO_3]$ + H_2O at 298 K: ♦, lactose; ▬, Fitting of experimental data by eq. 1**.**

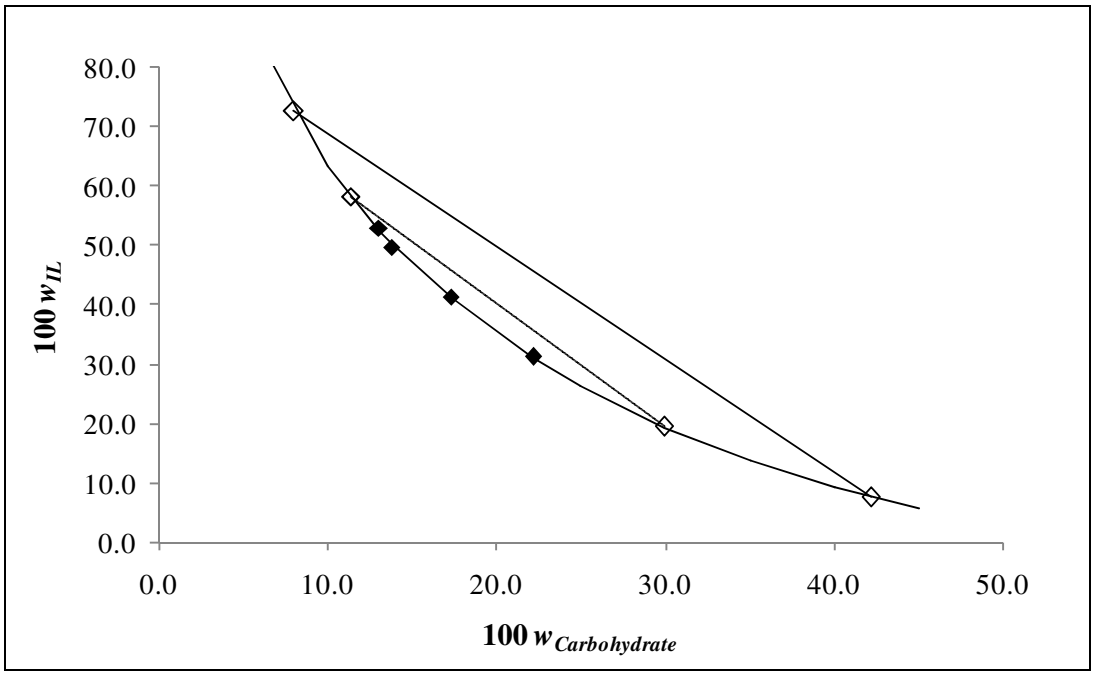

Figure E 6 - Phase diagram for L-(+)-arabinose based ternary systems composed by Saccharides + $[C_4mim][CF_3SO_3]$ + H_2O at 298 K: ♦, L-(+)-arabinose; ◊, TL data; ▬, Fitting of experimental data by eq. 1**.**

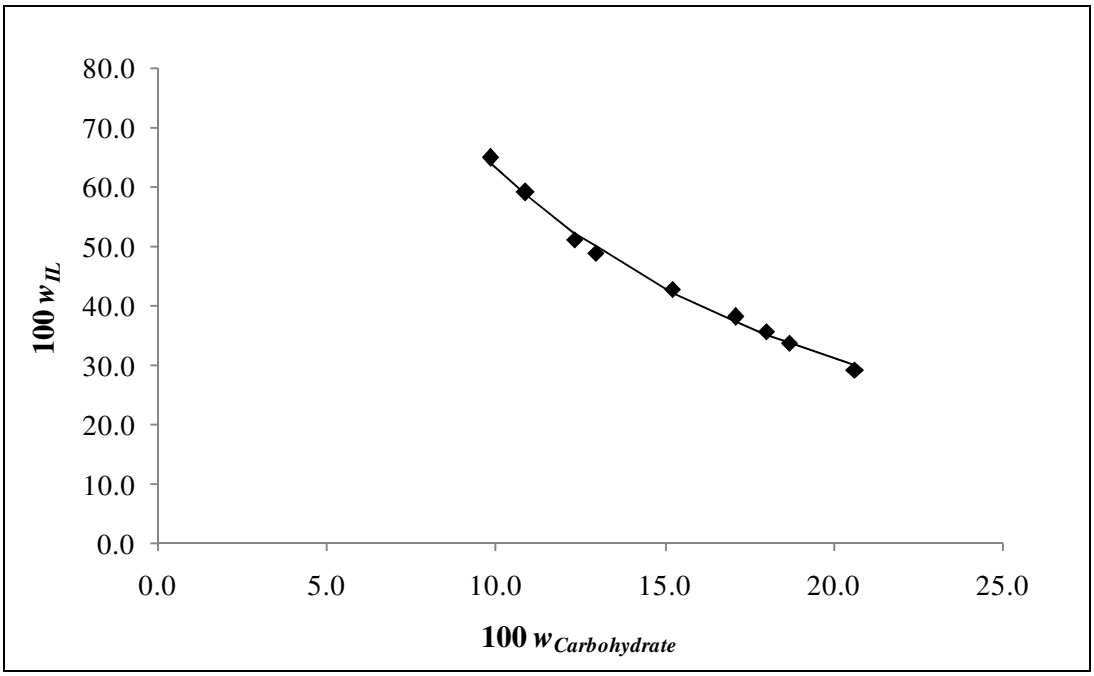

Figure E 7 - Phase diagram for D-(-)-arabinose based ternary systems composed by Saccharides + $[C_4mim][CF_3SO_3]$ + H_2O at 298 K: ♦, D-(-)-arabinose; ▬, Fitting of experimental data by eq. 1**.**

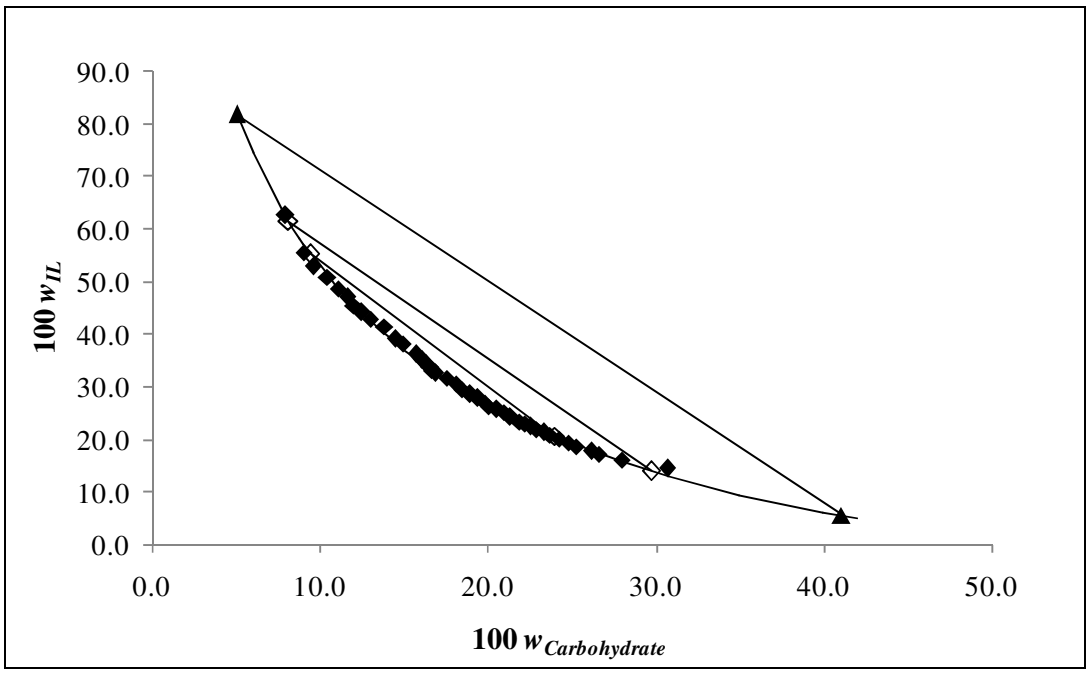

Figure E 8 - Phase diagram for xylitol based ternary systems composed by Saccharides + $[C_4mim][CF_3SO_3]$ + H_2O at 298 K: ♦, xylitol; ▲, extraction TL data; ◊, TL data; ▬, Fitting of experimental data by eq. 1.

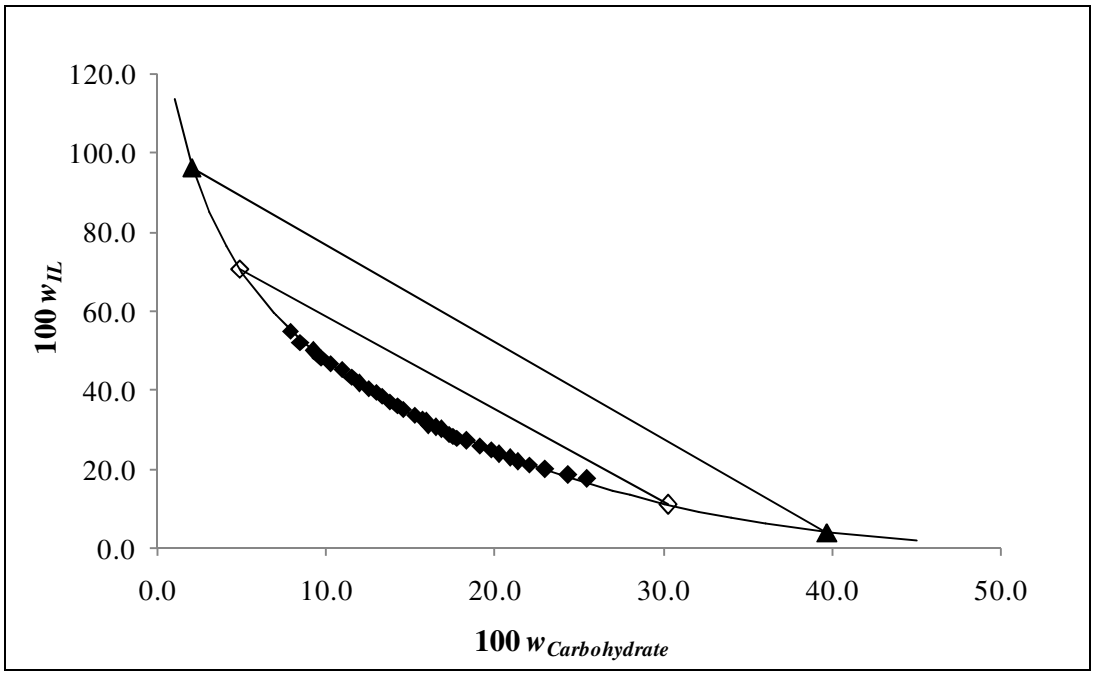

Figure E 9 - Phase diagram for maltitol based ternary systems composed by Saccharides + $[C_4mim][CF_3SO_3]$ + H_2O at 298 K: ♦,maltitol; ▲, extraction TL data; ◊, TL data; ▬, Fitting of experimental data by eq. 1.

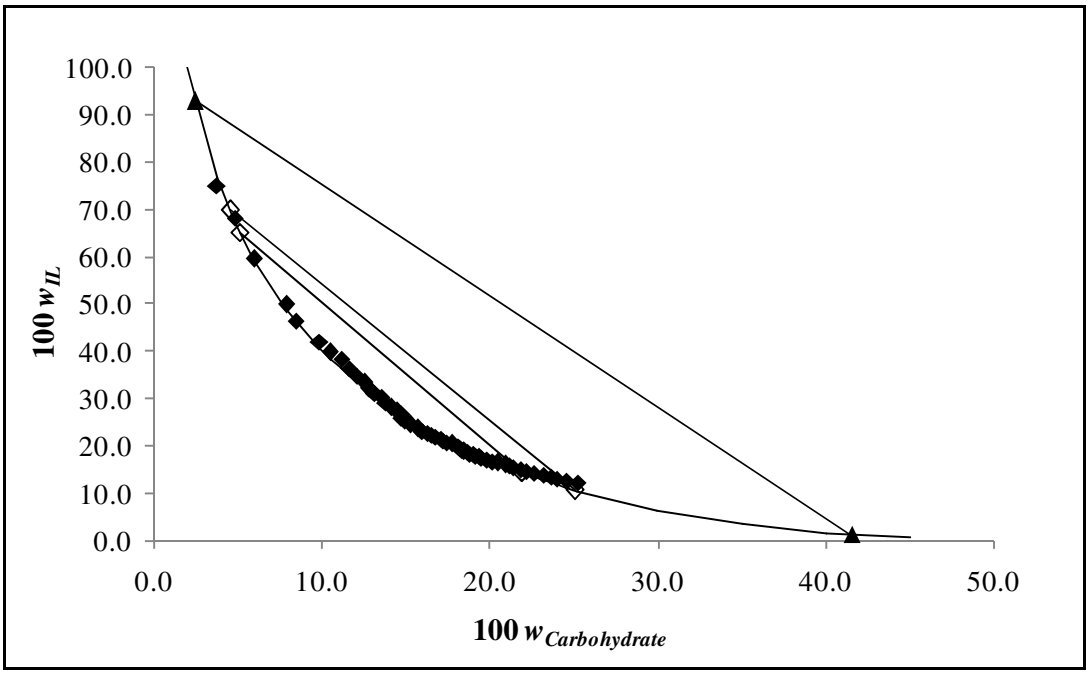

Figure E 10 - Phase diagram for D-sorbitol based ternary systems composed by Saccharides + $[C_4mim][CF_3SO_3]$ + H_2O at 298 K: ♦, D-sorbitol; ▲, extraction TL data; ◊, TL data; ▬, Fitting of experimental data by eq. 1.